

Investigation of Numerical Robustness and Dispersion Characteristics in Partition of Unity Finite Element Method for Helmholtz Equation Solutions

Maria J. Rodriguez-Alvarez, Sofia M. Sanchez-Castro

Department of Mathematical Sciences, University of Cantabria, Santander, Spain; Department of Applied Mathematics, Instituto de Matematicas de la Universidad de Salamanca, Salamanca, Spain

Abstract

The Partition of Unity Finite Element Method (PUFEM) has been widely used for the numerical simulation of the Helmholtz equation in different physical settings. In fact, it is a numerical pollution-free alternative method to the classical piecewise polynomial-based finite element methods. Taking into account a plane wave enrichment of the piecewise linear finite element method, the main goal of this work is focused on the derivation of the numerical dispersion relation and the robustness analysis of the PUFEM discretization when a spurious perturbation is presented in the wave number value used in the enrichment definition. From the one-dimensional Helmholtz equation, the discrete wave number is estimated based on a Bloch's wave analysis and *a priori* error estimates are computed explicitly in terms of the mesh size, the wave number, and the perturbation value.

Indexed keywords: Partition of unity finite element method; Discrete dispersion relation; robustness analysis

Article History: Received: 11 March 2025 | Accepted: 25 May 2025 | Published: 19 June 2025

1. Introduction

The accurate numerical simulation of time-harmonic wave propagation phenomena has been one of the most challenging goals over the last decades [16, 29] due to the oscillating behavior of the related solutions at the middle and high-frequency regime. In fact, the Helmholtz equation represents the prototypical model of this kind of phenomena



© 2025 The Authors. Open Access under CC BY 4.0.

How to cite: Maria J. Rodriguez-Alvarez, Sofia M. Sanchez-Castro (2025). Investigation of Numerical Robustness and Dispersion Characteristics in Partition of Unity Finite Element Method for Helmholtz Equation Solutions. Journal of Computer Engineering, 14(6), 60–87. DOI: <https://doi.org/10.5281/zenodo.19357514>

arising in different fields such as acoustics [10], electromagnetics [3], mechanics [19], or hydrodynamics [14], among many others.

The numerical simulation of the Helmholtz's like models can be performed by means of finitedifference methods [34], spectral methods [33], boundary element methods [24] or finite element methods [17, 18, 37] (both in h and hp -versions). Any of these methods suffer at some extent of the so-called phenomenon of numerical pollution [5], which corrupts the accuracy of these numerical methods when the wave number value is high, or the points per wavelength used in the discretization are not enough to guarantee that the asymptotic regime of the expected theoretical convergence is reached.

In the particular case of standard polynomial-based Galerkin approximations when they are applied to Helmholtz's like equations, there exist a variety of numerical methods which explicitly use particular solutions of the Helmholtz model such as [4, 7, 21, 36] to modify the discrete space including on it oscillatory functions such as plane waves. Among this type of so-called pollutionfree methods, the Partition of the Unity Finite Element Method [26] has been utilized in a wide variety of time-harmonic wave propagation problems (see for instance, [15, 20, 23]).

The computational advantages of the PUFEM method have been illustrated numerically by using different enrichment procedures (see, e.g. [25]) as well as its ill-conditioned behavior for low values of the wave number or for using a refined mesh as a partition of unity (see for instance [27, 38] among others). Despite these detailed numerical studies, the theoretical analysis of this partition of unity methods has been only developed partially. More precisely, after the PUFEM method was introduced in the middle nineties, some *a priori* error estimates were obtained [25] and later, related to Vekua's theory, plane wave approximations have been analyzed in [28], all of them without an explicit treatment of the error estimates in terms of the wave number value.

All these previous studies have been mainly based on the fact that a constant wave number value is *a priori* known without the presence of any spurious errors. However, if either heterogeneous materials are considered or uncertainties are assumed in the data of the Helmholtz model, then the wave number value could contain a perturbation error, which would affect the accuracy of the enrichment used to define the PUFEM method. For instance, this case is relevant in the structural analysis of three-dimensional trusses or framed structures [30], where the elastic properties of each beam component suffer spatial variations due to the aging processes of the materials.

As far as the author's knowledge goes, there is not any theoretical study of the PUFEM method (and, in general, for any other enriched pollution-free methods), where an error analysis is provided when the enriched functions present spurious perturbations in their definition. Consequently, the present work represents a stepping stone to the full analysis of the PUFEM method in higher dimensions.

In summary, in the present work, the plane wave enrichment of the PUFEM method is introduced by assuming a spurious perturbation error on the wave number value for the one-dimensional Helmholtz equation. In this setting, once the discrete Green function associated with the PUFEM discrete problem is computed explicitly, the discrete

dispersion relation is obtained. The robustness of the PUFEM method is studied by deriving error estimates expressed explicitly in terms of the mesh size, the wave number, and the perturbation value. With this purpose, a global interpolation procedure (based on a pre-asymptotic interpolation-like operator and a P_2 -polynomial based interpolant) for highly-oscillatory functions and a partial orthogonalization of the discrete space (which splits the PUFEM discrete space between vertex-value functions and *twin-bubble* functions) has been derived.

The structure of this manuscript is organized as follows: The one-dimensional Helmholtz boundary-value problem with Dirichlet and Robin boundary conditions is described in Section 2, as well as its variational formulation and the associated *inf-sup* condition. The PUFEM discretization is discussed in detail in Section 3. Then, a discrete *inf-sup* condition is proved (based on a global condensation procedure and the study of the discrete dispersion relation), and the existence and uniqueness of the discrete solution and its stability with respect to the boundary data are obtained in Section 4. An error estimate for the PUFEM is deduced in Section 7. Finally, some numerical results are presented in Section 8. The extension of the proposed analysis to higher dimensions and the conclusions are included in Sections 9 and 10, respectively. The interpolation estimates for the PUFEM discrete space in Appendix A.

2. Model problem

The time-harmonic wave propagation in isotropic homogeneous compressible media is modeled linearly by means of the Helmholtz equation. Throughout this work, a one-dimensional model will be studied. Without loss of generality, the computational domain is considered as the interval $(0,1)$ (otherwise, a change of scale could be performed to transform the domain into the unit interval). Analogously to the model problem used in [17] for the FEM analysis, the following boundary-value problem is analyzed:

$$\begin{aligned} -\Delta u - k^2 u &= f && \text{in } (0,1), \\ u(0) &= u_0, && (1) \\ u'(1) - iku(1) &= u_1, \end{aligned}$$

where u and f are complex-valued functions. The source term f is assumed to be independent of k . The boundary data $u_0, u_1 \in \mathbb{C}$ and the wave number $k > 0$ are constant. From an acoustic point of view, u could be understood as the complex-valued time-harmonic amplitude of the pressure field in a compressible fluid at a fixed wave number k .

Since a Dirichlet boundary condition is assumed at $x=0$ and a complex-valued Robin condition is imposed at $x=1$, it is straightforward to check that the model problem has a unique solution. Also, the boundary data u_0 and u_1 can be considered null without loss of generality (otherwise, a lift by a smooth function could be used to translate the solution). Hence, the solution will belong to the space

$$V = \{v \in H^1(0,1); v(0) = 0\} = H_{(0)}^1(0,1),$$

and so the variational formulation of problem (1) with homogeneous boundary conditions can be written as follows:

$$\begin{aligned} & \text{Find } u \in V \text{ such that } \forall v \in V, \\ & B_k(u, v) - ik u(1) \bar{v}(1) = \int_0^1 f(x) \bar{v}(x) dx \end{aligned} \quad (2)$$

where the sesquilinear form $B_k: V \times V \rightarrow \mathbb{C}$ is defined by

$$B_k(u, v) = \int_0^1 (u'(x) \bar{v}'(x) - k^2 u(x) \bar{v}(x)) dx, \quad u, v \in V. \quad (3)$$

The *inf-sup* condition on the sesquilinear form $(u, v) \mapsto B_k(u, v) - ik u(1) \bar{v}(1)$ ensures the existence and uniqueness of solution for problem (2) and the continuous dependence with respect to the data. It can even be shown that this condition can be obtained explicitly in terms of the wave number k (see [17]). Then, it holds the stability estimate $\|u\|_1 \leq Ck(\|f\|_0 + \|u_1\|)$, being $C > 0$ a constant independent on k .

3. PUFEM discrete problem

Following [26]: the PUFEM technique is introduced as a Galerkin method where the basis is obtained by multiplying Finite Element (FE) functions by some oscillatory terms, acting at a frequency close to the expected frequency in the solution of the problem. Then, as a first key component, an equispaced mesh is considered, this is,

$$T_h = \{x_j = hj : j = 0, \dots, n\} \subset [0, 1], \quad (4)$$

consisting of $n+1$ nodes with mesh size $h = 1/n$, and its related standard Lagrange P_1 FE basis. For the second key component in the PUFEM discretization (see [25, 31]), plane wave solutions of the homogeneous Helmholtz equation will be used. However, in the present work, instead of working with exact solutions of the Helmholtz equation (which would not be known in closed-form for time-harmonic problems with spatially dependent wave numbers), an additional perturbation parameter δ is introduced in these functions, in order to reproduce a lack of knowledge on the exact solutions. Hence, the perturbed plane waves used to describe the PUFEM discrete space are $e^{i(k+\delta)x}$ and $e^{-i(k+\delta)x}$. Consequently, the discrete functions are given by

$$\Psi_j^-(x) = \varphi_j(x) e^{-i(k+\delta)(x-x_j)}, \quad \Psi_j^+(x) = \varphi_j(x) e^{i(k+\delta)(x-x_j)} \quad \text{for } j = 0, \dots, n,$$

where $\{\varphi_j\}_{j=0}^n$ are the canonical basis functions of the P_1 -Lagrange FE discrete space. So, the functional spaces are defined by

$$X_h = \langle \{\psi_j^-\}_{j=0}^n \cup \{\psi_j^+\}_{j=0}^n \rangle, \tag{5}$$

$$V_h = \{v_h \in X_h; v_h(0) = 0\} = X_h \cap H_{(0)}^1(0, 1). \tag{6}$$

In this manner, the discrete PUFEM approximation, u_h , is defined as the solution of the following linear problem:

$$\begin{aligned} \square \square \square \text{Given } f \in L^2(0,1), \text{ find } u_h \in V_h \text{ such that} \\ \int_0^1 f(x) v_h^-(x) dx \quad \forall v_h \in V_h. \end{aligned} \tag{7}$$

$$\int_0^1 B_k(u_h, v_h) - i k u_h(1) v_h^-(1) = 0$$

3.1. Trigonometric discrete basis

The exponential terms in V_h can be split and rewritten, for any $v_h \in X_h$,

$$v_h(x) = \sum_{j=0}^n \left(v_{hj}^v \phi_j(x) \cos((k + \delta)(x - x_j)) + v_{hj}^b \phi_j(x) \sin((k + \delta)(x - x_j)) \right) \tag{8}$$

where $v_{hj}^v, v_{hj}^b \in \mathbb{C}$. As it is usual in a finite element framework, the description of the finite element discrete space is made by means of the writing the discrete functions in terms of the local expressions in the element of reference. Taking into account the affine transformation $F_j: T^{\wedge} \rightarrow T_j$ from the reference element $T^{\wedge} = [0,1]$ onto the finite element $T_j = [x_{j-1}, x_j]$, given by $F_j(x^{\wedge}) = h(x^{\wedge} + j - 1)$, with $x^{\wedge} \in [0,1]$, then the discrete PUFEM space X_h can be defined by $\{\psi_j^v\}_{j=0}^n \cup \{\psi_j^b\}_{j=0}^n$ where $\psi_j^v|_{T_{j+1}} \circ F_{j+1}(\hat{x}) = (1 - \hat{x}) \cos((k + \delta)h\hat{x})$ and $\psi_j^b|_{T_{j+1}} \circ F_{j+1}(\hat{x}) = (1 - \hat{x}) / ((k + \delta)h) \sin((k + \delta)h\hat{x})$ for $j = 0, \dots, n-1$. Analogous expressions hold for the restrictions of these functions in the element T_j . Then, $V_h = V_h^v \oplus V_h^b$ where $V_h^v = \langle \{\psi_j^v\}_{j=1}^n \rangle$ and $V_h^b = \langle \{\psi_j^b\}_{j=0}^n \rangle$. Due to the definition

of $\{\psi_j^v\}_{j=1}^n$, the degrees of freedom associated with those functions v_h in V_h^v are the values on the vertices of the mesh. In fact, it holds

$$v_h = \sum_{j=1}^n v_h(x_j) \psi_{vj}, \quad \forall v_h \in V_h^v.$$

Due to the relation written above, the discrete space V_h^v will be called *vertex-valued* discrete space. Also, notice that the functions $v_h^b \in V_h^b$ are null at all the vertices of the mesh. However, the basis $\{\psi_j^b\}_{j=0}^n$ of this discrete space V_h^b does not behave as the typical polynomial bubble basis in standard piecewise continuous P^p -finite elements with $p \geq 2$.

In that classical case, each discrete function in the basis of the polynomial bubble subspace could be non-null only in an unique element mesh T_j . More precisely, in this PUFEM discretization, the bubble functions $\{\Psi_j^b\}_{n_j=0}$ extend their support to two adjacent elements $T_j \cup T_{j+1}$, and at the interior of each element, its local shape resembles the classical polynomial bubbles (with opposite sign in each element). For this reason, the space V_h^b is called *twin-bubble* discrete space.

Remark 3.1. A similar decomposition can be performed in higher dimensions, splitting the discrete space in two different spaces: the subspace generated by nodal basis functions, whose degrees of freedom can be identified to their pointwise values at the vertices of the mesh, and the other discrete subspace containing the discrete functions which are null at all the vertices of the mesh. In the later case, the dimension of this bubble-like subspace will depend on the number of plane-waves used to enrich the PUFEM discretization. More precisely, in the two-dimensional case, once a preferred angles of incidence are chosen, $\theta_l, l = 0, \dots, M$, typically uniformly distributed in $[0, 2\pi)$, a discrete PUFEM function $v_h \in V_h$ is given by

$$v_h(\tilde{x}) = \sum_{j=0}^n \sum_{l=0}^M \phi_j(\tilde{x}) e^{i \tilde{k}_l \cdot \tilde{x}},$$

with $\tilde{k}_l = (k + \delta)(\cos\theta_l, \sin\theta_l)$. In this case, the dimension of the PUFEM discrete X_h is $(n + 1)(M + 1)$, and its splitting into two subspaces of vertex-valued and bubble-like functions have dimensions of $n+1$ and $(n+1)M$, respectively.

4. Global condensation procedure

Before the derivation of *a priori* error estimates for PUFEM, it should be ensured the existence and uniqueness of solution of the discrete problem (7), what cannot be addressed straightforward within the discrete functional setting introduced above. In the following sections, the space of the twin-bubble functions and the vertex-valued functions will be used separately to decouple the discrete problem in two independent discrete problems. Throughout the entire manuscript, different assumptions have been used in lemmas and theorems. For the sake of conciseness, they are listed in what follows:

(H1) Assume $|\delta|/k \leq 1$, which means that the wave number perturbation δ introduces a relative error with respect to the exact wave number k smaller than 100%.

(H2) There exists a constant value $\varepsilon > 1$ such that the wave number $k > \varepsilon$.

(H3) There exists a constant value $0 < \alpha < 1$ such that $h(k + |\delta|) \leq \alpha$.

√

(H4) There exists a constant value $\beta > 0$ such that $\delta^4 h^4 < (1-\beta)/(2C^{\wedge})$, being C^{\wedge} the approximation constant involved in (A.17).

(H5) There exists a constant value $\varepsilon > 0$ such that $\varepsilon \leq h(k+\delta)$.

To mimic the local condensation procedure used in P^p -finite elements (see [18]), a similar orthogonal procedure will be applied to V_h . However, due to the non-empty intersection between the supports of the basis functions in the twin-bubble space V^{b_h} , it is not possible to compute this orthogonalization locally (in the interior of each element T_j). The condensation procedure is applied to a global problem stated in the whole domain $(0,1)$, introducing an unusual functional framework. Firstly, the H^1 -bubble space is defined by

$$H^1_{\mathcal{T}_h}(0,1) = \{v \in H^1(0,1) : v(x) = 0 \text{ for all } x \in T_h\}.$$

Analogously to the functional spaces $H^1_0(0,1)$ or $H^1_0(0,1)$, the space $H^1_{\mathcal{T}_h}(0,1)$ is a Hilbert space endowed with the inner product associated with the H^1 -seminorm $|\cdot|_1$.

Lemma 4.1. Under hypothesis (H3), if B_k is defined by (3) then the sesquilinear form given by $(u,v) \mapsto B_k(u,v) - iku(1)v^-(1)$ for all $u,v \in H^1_{\mathcal{T}_h}(0,1)$ is continuous, hermitian and coercive.

Proof. Firstly, since $u(1) = v(1) = 0$ for any $u,v \in H^1_{\mathcal{T}_h}(0,1)$ then it is clear that the sesquilinear form defined in the statement of the lemma coincides with B_k and hence it is hermitian ($B(u,v) =$

$B(v,u)$ for all $u,v \in H^1_{\mathcal{T}_h}(0,1)$). The continuity of B_k in $H^1_{\mathcal{T}_h}(0,1)$ follows directly from the continuity of B_k in $H^1_0(0,1)$. However, a sharper continuity constant (smaller than $1+k^2$) can be obtained as follows. If it is introduced $\hat{v}_j = v|_{T_j} \circ F_j$ defined in $(0,1)$ then for any fixed $u,v \in H^1_{\mathcal{T}_h}(0,1)$, it holds

$$\begin{aligned} & \left| \sum_{j=1}^n \int_{T_j} u'(x)\bar{v}'(x) - k^2 u(x)\bar{v}(x) \right| \\ |B_k(u,v)| &= \left| \sum_{j=1}^n \int_{T_j} \frac{dx}{h} \left[\hat{u}'_j(\hat{x})\bar{\hat{v}}'_j(\hat{x}) - (kh)^2 \hat{u}_j(\hat{x})\bar{\hat{v}}(\hat{x}) \right] \right| \leq \frac{1+(kh)^2}{h} \sum_{j=1}^n \|\hat{u}_j\|_{H^1_0(0,1)} \|\hat{v}_j\|_{H^1_0(0,1)} \\ & \leq \sqrt{2}(1+(kh)^2) |u|_{H^1_0(0,1)} |v|_{H^1_0(0,1)} \leq \sqrt{2}(1+\alpha^2) |u|_{H^1_0(0,1)} |v|_{H^1_0(0,1)}, \end{aligned}$$

where it has been used the H^1 -Cauchy-Schwarz estimate in the second inequality, the Poincaré

estimate $\|u\|_1 \leq P_{1+1}/\pi^2 \|u\|_0 < 2 \|u\|_0$ in the third inequality (see [18, Lemma 2.2]), and the n -dimensional Cauchy-Schwarz estimate in the first inequality, and hypothesis (H3) in the last inequality. In addition, notice that $u^0(x)$ denotes du/dx for $x \in T_j$ whereas \hat{u}^0_j denotes $d\hat{u}_j/d\hat{x}$ for $\hat{x} \in (0,1)$ and any $j = 1, \dots, n$.

The coercivity of form B_k is also deduced using similar arguments. More precisely, it holds

$$\begin{aligned}
 B_k(u,u) &= \sum_{j=1}^n \int_{T_j} (|u'(x)|^2 - k^2 |u(x)|^2) dx = \sum_{j=1}^n \int_{\hat{T}_j} (|\hat{u}'_j(\hat{x})|^2 - (kh)^2 |\hat{u}_j(\hat{x})|^2) d\hat{x} \\
 &\geq \frac{\pi^2 - \alpha^2}{h} \sum_{j=1}^n \int_0^1 |\hat{u}'_j(\hat{x})|^2 d\hat{x} = \frac{\pi^2 - \alpha^2}{\pi^2} \sum_{j=1}^n \|u\|_{H^1_0(T_j)}^2 = \frac{\pi^2 - \alpha^2}{\pi^2} \|u\|_{2H^1_0(0,1)}^2,
 \end{aligned}$$

where it has been used that $(kh)^2 < \alpha^2$ (from (H3)) is smaller than π^2 , which is the smallest eigenvalue of the second-order derivative $-d^2/d\hat{x}^2$ in $(0,1)$ (see [18, Lemma 2.2]). \square

In addition to the result stated above, the Lax-Milgram lemma also ensures the existence and uniqueness of solution of the variational problem: under assumption (H3), which leads to $hk \leq \alpha < \pi$, and given $f \in L^2(0,1)$, find $v \in H^1_{\mathcal{T}_h}(0,1)$ such that

$$B_k(v,\phi) = \int_0^1 f\phi \quad \text{for all } \phi \in H^1_{\mathcal{T}_h}(0,1). \tag{9}$$

From the coercivity of B_k and the Poincaré inequality $\|v\|_0 \leq \|v\|_1$, it is straightforward the estimate

$$\|v\|_1 \leq \frac{\pi^2}{\pi^2 - \alpha^2} \|f\|_0. \tag{10}$$

It is also clear from the definition of the twin-bubble space that $V^{b_h} \subset H^1_{\mathcal{T}_h}(0,1)$. Since B_k is coercive in $H^1_{\mathcal{T}_h}(0,1)$, it will also be coercive in V^{b_h} , and B_k defines an inner product in both spaces, equivalent to the product associated with the seminorm $|\cdot|_1$. Hence, under assumption (H3), the analogous discrete version of the problem (9): given $f \in L^2(0,1)$, find $v_b \in V^{b_h}$ such that

$$B_k(v_b,\phi_b) = \int_0^1 f\phi_b \quad \text{for all } \phi_b \in V^{b_h}, \tag{11}$$

has a unique solution, and it also holds

$$|v_b|_1 \leq \frac{\pi^2}{\pi^2 - \alpha^2} \|f\|_0. \quad (12)$$

Despite the previous estimates (in the continuous and discrete variational problems guarantees the well-posedness of both problems), the estimate (10) is not sharp and it can be improved as follows: taking into account that $H^1_{T_h}(0,1) = \prod_{j=1}^n H^1_0(T_j)$ (understanding that the inclusion of $H^1_0(T_j)$ in $H^1_0(0,1)$ is made by the extension by zero of those functions defined in $T_j \subset (0,1)$).

Lemma 4.2. Under hypothesis (H3) and given $f \in L^2(0,1)$, $v \in H^1_{T_h}(0,1)$ is a solution of problem (9) if and only if $v|_{T_j} = v_j$ is a solution of the problem

$$B_k(v_j, \phi) = \int_{T_j} f \phi, \text{ for all } \phi \in H^1_0(T_j). \quad (13)$$

with $j = 1, \dots, n$. In addition, it holds

$$|v|_1 \leq \frac{\pi^2}{\pi^2 - \alpha^2} h \|f\|_0. \quad (14)$$

Proof. The equivalence between problems (9) and (13) is immediate. Defining $v_j = v|_{T_j}$, taking test functions ϕ with compact support in T_j , and substituting in problem (9), then (13) is obtained. Reciprocally, if each v_j is extended by zero to the exterior of T_j , and then these extensions $\chi_{T_j} v_j$ are summed up, then $v = \sum_{j=1}^n \chi_{T_j} v_j$ is the solution of problem (9). To assess this statement, it is enough to use that any $\phi \in H^1_{T_h}(0,1)$ can be rewritten as $\phi = \sum_{j=1}^n \chi_{T_j} \phi_j$ with $\phi_j \in H^1_0(T_j)$, and add the variational formulations (13) from $j = 1$ to n .

To obtain a sharper estimate, the variational problem (13) is rewritten in the reference element $(0,1)$. Hence, it is obtained that $\hat{v}_j = v|_{T_j} \circ F_j$ is the solution of the variational problem

$$\int_0^1 \left(\hat{v}'_j(\hat{x}) \bar{\phi}'(\hat{x}) \, d\hat{x} - (kh)^2 \hat{v}_j(\hat{x}) \bar{\phi}(\hat{x}) \right) d\hat{x} = h^2 \int_0^1 (f|_{T_j} \circ F_j)(\hat{x}) \bar{\phi}(\hat{x}) \, d\hat{x},$$

for all $\phi \in H^1_0(T_j)$ with $j = 1, \dots, n$. The analogous estimate to (10), but now applied to a problem stated in T_j , leads to $|\hat{v}_j|_{H^1_0(0,1)} \leq \pi^2 / (\pi^2 - \alpha^2) h^2 \|f|_{T_j} \circ F_j\|_{L^2(0,1)}$ and coming back to T_j it is obtained $|v_j|_{H^1_0(T_j)} \leq \pi^2 / (\pi^2 - \alpha^2) h \|f|_{T_j}\|_{L^2(T_j)}$. Estimate (14) follows adding the squares of the left and right-hand side in the inequality written above from $j = 1, \dots, n$. \square

Remark 4.3. A similar analysis could be addressed in higher-dimensions following the steppingstone idea of global condensation presented above, taking into account that the bubble-like subspace V^{b_h} is going to be larger than in the one-dimensional case and the

fact that the functional space $H_{\mathcal{T}_h}^1(\Omega) = \{\phi \in H^1(\Omega) : \phi|_{\partial T} = 0, \forall T \in \mathcal{T}_h\}$ will involve functions which are null on the edges in two dimensional problems, or faces in the three-dimensional case. Notice that the classical condensation algorithm used in typical hp-fem discretizations [9] should be extended to the global setting proposed in this work and hence instead of using an elementwise orthogonalization procedure [35], global orthogonal relations should be considered as it has been already stated in the variational problem (16).

Since $V_h^{b_h}$ cannot be rewritten as a direct sum of the space of bubbles functions with support in each finite element T_j , the proof of Lemma 4.2 cannot be replicated for the discrete problem (11). However, despite this drawback, the estimate (12) for the discrete solution can also be improved by using that the error $v - v_b$ is orthogonal to $V_h^{b_h}$ with respect to the inner product B_k .

Lemma 4.4. Under hypothesis (H3) and given $f \in L^2(0,1)$, if $v_b \in V_h^{b_h}$ is the solution of problem (11), then it holds

$$|v_b|_1 \leq \sqrt{2}(1 + \alpha^2) \left(\frac{\pi^2}{\pi^2 - \alpha^2} \right)^2 h \|f\|_0 \quad (15)$$

Proof. From variational problems (9) and (11), it is clear that $B_k(v - v_b, \varphi_b) = 0$ for all $\varphi_b \in V_h^{b_h}$, or equivalently, $B_k(v_b, \varphi_b) = B_k(v, \varphi_b)$. If $\varphi_b = v_b$, taking into account the coercivity and the continuity of B_k (see Lemma 4.1), and also estimate (14), it holds

$$\frac{\pi^2 - \alpha^2}{\pi^2} |v_b|_1^2 \leq |B_k(v_b, v_b)| = |B_k(v, v_b)| \leq \sqrt{2}(1 + \alpha^2) |v_b|_1 |v|_1 \leq \frac{\sqrt{2}(1 + \alpha^2) \pi^2 h}{\pi^2 - \alpha^2} |v_b|_1 \|f\|_0.$$

Since it can be supposed that $|v_b|_1 > 0$ (otherwise $f = 0$ and the lemma follows immediately), the expression above leads to (15), simplifying the factor $|v_b|_1$ at the most right and most left terms of the inequalities written above. \square

For the subsequent parts of the existence and uniqueness results and the *a priori* error analysis, it will be useful to split the PUFEM discrete space as the direct sum $V_h = \tilde{V}_h \oplus V_h^{b_h}$ where the orthogonality is computed by means of the inner product induced by form B_k . With this purpose, for each ψ_j^v , it will be defined $\tilde{\psi}_j^v = \psi_j^v + \xi_j^{b_h}$ such that it is satisfied the orthogonal relation $B_k(\tilde{\psi}_j^v, \phi^b) = 0$ for all $\phi^b \in V_h^{b_h}$, or equivalently, find $\xi_j^{b_h} \in V_h^{b_h}$ such that

$$B_k(\xi_j^{b_h}, \phi^b) = -B_k(\psi_j^v, \phi^b) \text{ for all } \phi^b \in V_h^{b_h}. \quad (16)$$

Notice again that this orthogonalization procedure involves a global problem stated in the whole domain $(0,1)$ (whereas in the classical polynomial space it can be performed locally). Since B_k is a coercive form in $H_{\mathcal{T}_h}^1(0,1)$ and also in $V_h^{b_h}$, the application of the Lax-

Milgram lemma guarantees the existence and uniqueness of solution of problem (16), and the estimate (15) with $f = \psi^v_j \in$

$L^2(0,1)$ reads

$$|\xi_j^v|_1 \leq \sqrt{2}(1 + \alpha^2) \left(\frac{\pi^2}{\pi^2 - \alpha^2} \right)^2 h \|\psi_j^v\|_0. \tag{17}$$

In conclusion, the discrete PUFEM problem will be represented in terms of the partially orthogonal basis $\{\tilde{\Psi}_j^v\}_{j=1}^n \cup \{\Psi_j^b\}_{n_j=0}$, which induces the representation $V_h = V^{\sim v}_h \oplus V^b_h$.

Remark 4.5 (Invariant translation). Notice that, since the mesh is uniform (all the elements have the same length h), any discrete basis function in the trigonometric basis $\{\Psi_j^v\}_{j=1}^n \cup \{\Psi_j^b\}_{n_j=0}$ is invariant under translation, i.e., $\Psi_j^v(x) = \Psi_m^v(x - h(j - m))$ and $\psi^b_j(x) = \psi^b_m(x - h(j - m))$. Con-

sequently, the partial orthogonal basis $\{\tilde{\Psi}_j^v\}_{j=1}^n \cup \{\Psi_j^b\}_{n_j=0}$ also shares the same property since its functions are linear combination of the trigonometric basis functions. In addition, it is important to realize that $\psi^{\sim v}_j$ is symmetric with respect to $x = x_j$, i.e., $\tilde{\Psi}_j^v(x_j + s) = \tilde{\Psi}_j^v(x_j - s)$ for $0 \leq s \leq h$.

Such symmetry property does not hold for the twin-bubble functions ψ^b_j .

Now, taking into account this orthogonal relation between the different basis functions and its invariant translation property, problem (7) admits the matrix representation

$$L_h \vec{u}_h = \vec{f}_h, \tag{18}$$

where $\vec{u}_h = (\vec{u}_h^v, \vec{u}_h^b) = (u_1^v, \dots, u_n^v, u_0^b, \dots, u_n^b)^t$ are the coefficients of the discrete solution $u_h \in V_h$, given by

$$u_h = \sum_{j=1}^n u_j^v \tilde{\Psi}_j^v + \sum_{j=0}^n u_j^b \psi_j^b,$$

and the matrix L_h (of size $(2n+1) \times (2n+1)$) is defined by blocks as follows:

$$L_h = \begin{pmatrix} 0 & L_{(n+1)h^v} \times n & 0 & n \times L_{(nh^b+1)} \end{pmatrix},$$

where the $n \times n$ matrix L_h^v and the $(n+1) \times (n+1)$ matrix L_h^b are given by

$$\begin{pmatrix} \text{?} & R_h & \text{?} & \text{?} & \text{?} \\ 2S_h & 2S_h & R_h & \text{?} & \text{?} \\ \text{?} & \text{?} & S_{1h} & S_b + S_b & R_b \\ \text{?} & \text{?} & \text{?} & \text{?} & \text{?} \end{pmatrix}$$

seminorm $|\cdot|_{1,fe}$ for a vector of point-wise values $\sim v = (v_1, \dots, v_n)^t$ associated to a finite element function $v_{fe} = \sum_{j=1}^n v_j \Phi_h$ are defined as follows:

$$k v_{fe}^k_{L^2(0,1)} = k \sim v^k_{0, V_{feh}} = \left(h \sum_{j=1}^n |v_j|^2 \right)^{\frac{1}{2}}, \quad |v_{fe}|_{H^1(0,1)} = |\vec{v}|_{1, V_{feh}} = \left(h \sum_{j=1}^n \left| \frac{v_j - v_{j-1}}{h} \right|^2 \right)^{\frac{1}{2}}, \quad (22)$$

where it is assumed that $v_0 = 0$ (due to the homogeneous Dirichlet condition at $x = 0$). Analogously, the PUFEM norms associated to a function $v_h = \sum_{j=1}^n v_j \tilde{\Psi}_j^v \in V_{h^v}$ associated to its pointwise value vector $\sim v = (v_1, \dots, v_n)$ are defined by

$$\|v_h\|_{L^2(0,1)} = \|\vec{v}\|_{0, \tilde{V}_h^v} = \left(\vec{v}^{*} \tilde{\mathcal{M}}_h \vec{v} \right)^{\frac{1}{2}}, \quad |v_h|_{H^1(0,1)} = |\vec{v}|_{1, \tilde{V}_h^v} = \left(\vec{v}^{*} \tilde{\mathcal{K}}_h \vec{v} \right)^{\frac{1}{2}}, \quad (23)$$

where $[\tilde{\mathcal{M}}_h]_{jl} = \int_0^1 \tilde{\Psi}_j^v \tilde{\Psi}_l^v dx$ and $[\tilde{\mathcal{K}}_h]_{jl} = \int_0^1 (\tilde{\Psi}_j^v)' (\tilde{\Psi}_l^v)' dx$, and again it has been assumed that $v_0 = 0$.

Although any pair of norms are equivalent in a finite-dimensional space, the following lemma states the equivalence constants independently of h , k , and δ .

Lemma 4.6. *Under hypothesis (H3), if $v_h = \sum_{j=1}^n v_j \tilde{\Psi}_j^v \in V_{h^v}$ and $\sim v = (v_1, \dots, v_n)$ is its point-wise value vector, then it holds*

$$C_1 k \sim v^k_{0, V_{feh}} \leq k v_h^k_{L^2(0,1)} \leq C_2 k \sim v^k_{0, V_{feh}}, \quad C_1 |\sim v|_{1, V_{feh}} \leq |v_h|_{H^1(0,1)} \leq C_2 |\sim v|_{1, V_{feh}}, \quad (24)$$

where C_1 and C_2 are positive constant functions independent of h , k , and δ (depending only on α).

Proof. It will be followed by a slight modification of the steps used in [11, Lemma 9.7] to prove the equivalence of norms in polynomial finite element spaces between the discrete functions and its point-wise value vectors.

Clearly, if $v_h \in V_{h^v}$ then $\hat{v}_j = v_h|_{T^o \circ F_j}$ for any fixed $j = 1, \dots, n$ belongs to the span of local functions $\langle \tilde{\Psi}_{j-1}^v|_{T_j^o \circ F_j}, \tilde{\Psi}_j^v|_{T_j^o \circ F_j} \rangle^j$ defined by the partially orthogonal procedure. Hence, \hat{v}_j defined in T^{\wedge} is represented by the C^2 -coordinate basis vector $\sim v_j = (v_{j-1}, v_j)^t$. Direct inspection reveals that the two local functions $\{\tilde{\Psi}_{j-1}^v|_{T_j^o \circ F_j}, \tilde{\Psi}_j^v|_{T_j^o \circ F_j}\}$ depend continuously on the parameter $h(k+\delta) \in (0, \alpha]$ (which holds under assumption (H3)). Consequently, if K^{\wedge}_{loc} and M^{\wedge}_{loc} denote the local stiffness and mass matrices defined in T^{\wedge} with respect to this local PUFEM basis, then the coefficients of these matrices also depend continuously on the parameter $h(k+\delta)$. In addition, if

$K^{\wedge}_{loc^{fe}}$ and $M^{\wedge}_{loc^{fe}}$ denote the analogous local stiffness and diagonal lumped mass matrices ($M^{\wedge}_{loc^{fe}}$ is equal to the 2×2 identity matrix) with respect to this local standard piecewise P^1 -FE basis, then it holds

$$\lambda_{\min}(h(k+\delta)) \leq \frac{\sim v^* j M^{\wedge}_{loc} \sim v j}{\mu_{\max}(h(k+\delta)), \sim v^* j M^{\wedge}_{loc^{fe}} \sim v j} \leq \lambda_{\max}(h(k+\delta)), \quad \mu_{\min}(h(k+\delta)) \leq \frac{\sim v^* j K^{\wedge}_{loc} \sim v j}{\sim v^* j M^{\wedge}_{loc^{fe}} \sim v j} \leq$$

where $\lambda_{\min}(h(k + \delta))$ and $\lambda_{\max}(h(k + \delta))$ are respectively the minimum and maximum eigenvalues of the symmetric generalized eigenvalue problem $K^{\wedge}_{loc} \sim v = \lambda K^{\wedge}_{loc^{fe}} \sim v$, and $\mu_{\min}(h(k + \delta))$ and $\mu_{\max}(h(k + \delta))$ are respectively the minimum and maximum eigenvalues of the symmetric generalized eigenvalue problem $M^{\wedge}_{loc} \sim v = \mu M^{\wedge}_{loc^{fe}} \sim v$. In both cases, their eigensolutions also depend continuously on the parameter $h(k+\delta)$. Hence, the maps $h(k+\delta) \mapsto \lambda_{\min}(h(k+\delta))$ and $h(k+\delta) \mapsto \lambda_{\max}(h(k+\delta))$ are continuous functions defined in a non-empty compact domain $[0, \alpha]$. So, using the Weierstrass theorem, both continuous functions reach respectively a minimum λ_{\min} and a maximum value λ_{\max} (possibly depending on α). The same argument should be applied to bound the eigenvalues $\mu_{\min}(h(k+\delta))$ and $\mu_{\max}(h(k+\delta))$.

Now, taking into account that $\sim v^* j M^{\wedge}_{loc^{fe}} \sim v j = |v_{j-1}|^2 + |v_j|^2$ and $\sim v^* j K^{\wedge}_{loc^{fe}} \sim v j = |v_j - v_{j-1}|^2$, and the

fact that $\|j\|_{L^2(\hat{T})}^2 = \tilde{v}^* j M^{\wedge}_{loc} \sim v j$, and $|\hat{v}_j|_{H^1(\hat{T})}^2 = \sim v^* j K^{\wedge}_{loc} \sim v j$, it holds

$$\lambda_{\min}(|v_{j-1}|^2 + |v_j|^2) \leq \|\hat{v}_j\|_{L^2(\hat{T})}^2 \leq \lambda_{\max}(|v_{j-1}|^2 + |v_j|^2),$$

$$\mu_{\min} |v_j - v_{j-1}|^2 \leq |\hat{v}_j|_{H^1(\hat{T})}^2 \leq \mu_{\max} |v_j - v_{j-1}|^2.$$

and coming back to element T_j by applying the affine transform F_j , using that $|v_h|_{T_j}|_{H^1(T_j)} = |\hat{v}_j|_{H^1(\hat{T})}/h$ and $\|v_h|_{T_j}\|_{L^2(T_j)}^2 = h \|\hat{v}_j\|_{L^2(\hat{T})}^2$, the estimate written above leads to

$$\lambda_{\min} h(|v_{j-1}|^2 + |v_j|^2) \leq \|v_h|_{T_j}\|_{L^2(T_j)}^2 \leq \lambda_{\max} h(|v_{j-1}|^2 + |v_j|^2),$$

$$\frac{\mu_{\min} |v_j - v_{j-1}|^2}{h} \leq \frac{\|v_h|_{T_j}\|_{H^1(T_j)}^2}{h} \leq \mu_{\max} |v_j - v_{j-1}|^2.$$

If the terms in the previous inequality are added from $j = 1$ to n and the root square is computed, estimates (24) are obtained. \square

5. Discrete dispersion relation

The derivation of discrete dispersion relations for the discrete linear system can be made identifying those Bloch discrete waves in V_h , which are homogeneous solutions of the discrete Helmholtz problem on the uniform mesh. In what follows, estimates of the difference between the continuous and the discrete wave number will be derived using similar arguments to those one described in [18].

To write the discrete Green's function associated with the discrete PUFEM problem (21), the first step consists in the estimation of the discrete wave number. More precisely, the wave number associated with the exact solution of the homogeneous Helmholtz equation will be compared with those solutions which satisfy the row equations of the tridiagonal matrix L_h^v , stated in a uniform mesh extended throughout the whole real line.

With this comparative aim, first, an exact tridiagonal stencil L_h^{ex} will be computed in such a manner that the Bloch plane waves with exact wave number k satisfy this *exact* stencil. So, instead of using the discrete basis $\{\tilde{\Psi}_j^v\}_{n_j=1}$ in $V_{h^v} \subset H_{(0)}^1(0, 1)$, the set of linearly independent functions

$\{u_j\}_{n_j=1}$ in $H_{(0)}^1(0, 1)$ is considered, which are defined as the unique solution of the continuous Helmholtz problem:

$$\begin{aligned} (-u'' - k^2 u) &= 0 && \text{in } T_{j-1} \cup T_j = [x_{j-1}, x_{j+1}], \\ u(x_{j-1}) &= 0, && u(x_j) = 1, && u(x_{j+1}) = 0. \end{aligned} \quad (25)$$

Inserting this set of functions in the variational problem (2) (without taking into account the boundary conditions), the tridiagonal stencil, which is obtained for the interior nodes (for $j = 1, \dots, n-1$), satisfies

$$R_{ex} u_{ex}(x_{j+1}) + 2S_{ex} u_{ex}(x_j) + R_{ex} u_{ex}(x_{j-1}) = 0, \quad (26)$$

where u_{ex} is an exact solution of the homogeneous Helmholtz equation and S_{ex} and R_{ex} are given by

$$2S_{ex} = B_k(u_j, u_j), \quad R_{ex} = B_k(u_j, u_{j+1}) = B_k(u_j, u_{j-1}). \quad (27)$$

Since $u_{ex}(x) = Ae^{ikx} + Be^{-ikx}$ with $A, B \in \mathbb{C}$, the fundamental Bloch solutions of (26) are

$$u^+_h(k; x) = \sum_{j \in \mathbb{Z}} u_j(x) e^{ikxj}, \quad u^-_h(k; x) = \sum_{j \in \mathbb{Z}} u_j(x) e^{-ikxj}, \quad (28) \quad j \in \mathbb{Z}$$

and consequently

$$\cos(kh) = - \frac{S_{ex}}{R_{ex}}. \quad (29)$$

R_{ex}

The next step in the derivation of the discrete wave number for the PUFEM discretization in $V^{\sim}_h{}^v$ consists in the statement of an equivalent variational formulation associated to problem (25). Since u_j is defined piecewise in each element T_j and T_{j+1} , it can be rewritten as the addition of a basis function in V^v_h plus a function of the H^1 -bubble space. Hence, given $\psi^v_j \in V^v_h$, the exact solution

$u_j = \psi^v_j + \xi_j \in V^v_h \oplus H^1(0,1)_{T_h}$ is determined by means of the solution of the variational problem

$$B_k(\xi_j, \phi) = -B_k(\psi^v_j, \phi) \text{ for all } \phi \in H^1_{T_h}(0,1) \quad \text{for } j = 1, \dots, n. \quad (30)$$

Using Lemma 4.1, if hypothesis (H3) holds then the problem stated above has a unique solution since B_k is continuous and coercive in $H^1_{T_h}(0,1)$. It should be remarked that the variational problem (30) is the continuous version of the discrete variational problem (16), where the partially orthogonal basis $\{\tilde{\Psi}^v_j\}_{j=1}^n$ was defined by means of the computation of $\{\xi^b_j\}_{j=1}^n \subset V^v_h \subset H^1_{T_h}(0,1)$.

It should also be noticed that the form B_k has real-valued coefficients, and hence, since the righthand side of problems (30) and (16) are defined by real-valued functions (as in the case of functions $\{\psi^v_j\}_{j=1}^n$), then the solutions of these variational problems are also real-valued.

Lemma 5.1. *Under assumption (H3), if u_j , u_l and $\tilde{\Psi}^v_j$, $\tilde{\Psi}^v_l$ are defined respectively by the variational problems (30) and (16), then*

$$B_k(u_j - \tilde{\psi}^v_j, u_l - \tilde{\psi}^v_l) = B_k(\tilde{\psi}^v_j, \tilde{\psi}^v_l) - B_k(u_j, u_l), \quad (31)$$

for all $j, l = 1, \dots, n$.

Proof. The arguments used in this proof are completely analogous to those presented in [18, Lemma 3.1]. \square

Now, the attention must be focused on the discrete problem associated to the variational problem (21) stated in $V^{\sim}_h{}^v$. In that case, since the discrete functions $V^{\sim}_h{}^v$ are determined by their pointwise values at the vertices of the mesh, the tridiagonal stencil which is formally satisfied for a

Bloch wave $u_h(x) = \sum_{j \in \mathbb{Z}} \tilde{\Psi}^v_j(x) e^{ik_0 x j}$ leads to

$$R_h u_h(x_{j+1}) + 2S_h u_h(x_j) + R_h u_h(x_{j-1}) = 0, \quad (32)$$

where recall that S_h and R_h are given by $2S_h = B_k(\tilde{\Psi}^v_j, \tilde{\Psi}^v_j)$ and $R_h = B_k(\tilde{\Psi}^v_j, \tilde{\Psi}^v_{j-1})$. Hence, from (32)

it is obtained the discrete dispersion relation

$$\cos(k^\circ h) = -\frac{S_h}{R_h}, \quad (33)$$

being k° the so-called discrete wave number associated with the PUFEM discretization in V_h^v .

Remark 5.2. In the context of standard polynomial finite element methods, assuming an invariant translation of the mesh (for instance, using tensor-product meshes, Cartesian grids, etc.) analogous arguments have been used to obtain their dispersion relation in closed form (see for instance [1, 13]). Under the same considerations, the one-dimensional computations could be used as a stepping stone to obtain, with cumbersome analytical computations, the PUFEM dispersion relation in higher dimensions. More precisely, in the case of d -dimensional Cartesian rectangular grids, taking into account its tensor product structure, the fundamental Bloch solutions can be written as $U_h^\pm(x_1, \dots, x_d) = \prod_{r=1}^d u_h^\pm(k_r; x_r)$, where u_h^\pm is defined by (28). Hence, following analogous arguments to those used in [1, Section 2.3], it can be deduced that the dispersion relation in higher dimensions is given by

$$\sum_{r=1}^d (k_{r^\circ})_2 = (k^\circ)_2$$

where k_{r° is related by the wavenumber k by the one-dimensional dispersion relation (33).

Theorem 5.3. Under hypothesis (H1)-(H4), if k° is the discrete wave number defined in (33) then it holds

$$\begin{aligned} |\cos(kh) - \cos(k^\circ h)| &\leq C\delta^4 h^4, & |k^\circ - k| &\leq C\delta_4 h^2, \end{aligned} \quad (34)$$

where C is a positive constant independent of h , k , and δ (and only dependent on α and β).

Proof. The arguments used in this proof are almost identical to those ones used in [18, Theorem

3.2]. Firstly, straightforward computations show that u_j are defined by

$$\begin{aligned} &\square \\ &\square \square -\cot(kh)\sin(k(x-x_j)) + \cos(k(x-x_j)) \text{ for } x \in T_{j+1}, u_j(x) = \\ &\cot(kh)\sin(k(x-x_j)) + \cos(k(x-x_j)) \text{ for } x \in T_j, \end{aligned}$$

$$\square \square_0 \quad \text{otherwise.}$$

Then, direct computations show that

$$(35) \quad \|u_j\|_0^2 = h \left(\frac{2}{3} + O(k^2 h^2) \right) \quad |u_j|_1^2 = \frac{1}{h} (2 + O(k^2 h^2)) \quad ,,$$

and also

$$2S_{ex} = u_j = \frac{1}{B_k(u_j, -)} (2 + O(k^2 h^2)) \quad , \quad u_{j+1} = \frac{1}{B_k(u_j, -)} (-1 + O(k^2 h^2)) \quad R_{ex} = \quad (36) \quad h \quad h$$

where $O(k^2 h^2)$ must be read as a tailored expression bounded by $C_1 k^2 h^2 + C_2 k^4 h^4 + \dots$, where C_1, C_2, \dots are positive constants independent of k and h .

Using the discrete dispersion relations (29) and (33)

$$(37) \quad |\cos(kh) - \cos(k'h)| = \frac{h}{R_h} - \frac{\left| S_{ex} S_h R_{ex} - S_{ex} R_h \right|}{R_{ex} R_h R_{ex}}$$

In consequence, to estimate the difference between both cosines in the expression above, it is enough to obtain an upper bound for the numerator and a positive lower bound for the denominator.

First, it should be taken into account that $u_j|_{T_j}$ is the exact solution of a similar variational problem to (30), but with test functions in $H_0^1(T_j)$. In the same manner, the PUFEM approximation $\tilde{v}_j|_{T_j}$ is the exact solution of a similar variational problem to (16), but where the test functions used are in the discrete space $W^{b_j} = \{\phi^b|_{T_j} : \phi^b \in V_h^b\}$. Hence, estimates in Lemma A.6 can be applied for $h(k+\delta) < 2\pi$, taking into account the discretization space $\{\Psi_j^v|_{T_j}\} \cup W^{b_j}$. Due to the interpolatory properties of the global interpolant I_h (see Remark A.7), it holds that $I_h(u_j|_{T_j}) = \Psi_j^v|_{T_j} + \phi_I^b|_{T_j}$ with some $\phi_I^b \in V_h^b$. In this manner, utilizing Cea's lemma (see [8]) applied to the variational problems (30) and (16) rewritten in $H^1(T^)$, it holds

$$\begin{aligned} |u_j|_{T_j} - \tilde{\Psi}_j^v|_{T_j}|_{H^1(T_j)} &\leq \frac{\sqrt{2\pi^2(1+\alpha^2)}}{\pi^2 - \alpha^2} \inf_{b \in V^b} |u_j|_{T_j} - \psi_j^v|_{T_j} + \phi^b|_{T_j}|_{H^1(T_j)} \quad h \\ &\leq \frac{\sqrt{2\pi^2(1+\alpha^2)}}{\pi^2 - \alpha^2} |u_j|_{T_j} - I_h u_j|_{T_j}|_{H^1(T_j)} \leq C\delta^2 h^2 |u_j|_{T_j}|_{H^1(T_j)}. \end{aligned}$$

Adding the analogous estimation in T_{j+1} , it is obtained

$$|u_j - \tilde{\Psi}_j^v|_1 \leq C\delta^2 h^2 |u_j|_1 \text{ for all } j = 1, \dots, n, \tag{38}$$

being C a positive constant independent of h, k , and δ .

Second, the numerator in (37) can be estimated using Lemma 5.1, the continuity of B_k in $H^1 T_h$, the computations (36), and the estimate (38) as follows:

$$\begin{aligned} \frac{1}{2} |ShR_{ex} - S_{ex}Rh| &= |B_k(u_j, u_j)B_k(\psi^{\sim} v_j, \psi^{\sim} v_{j+1}) - B_k(u_j, u_{j+1})B_k(\psi^{\sim} v_j, \psi^{\sim} v_j)| \\ &\leq |B_k(u_j, u_j)| |B_k(u_j - \tilde{\Psi}_j^v, u_{j+1} - \tilde{\Psi}_{j+1}^v)| + |B_k(u_j, u_{j+1})B_k(u_j - \tilde{\Psi}_j^v, u_j - \tilde{\Psi}_j^v)| \\ &\leq (2 + O(hk)) \sqrt{2} \hat{C}^2 \delta^4 h^4 |u_j|_1 |u_{j+1}|_1 \leq \\ &\quad + \frac{1}{h} (1 + O(h^2 k^2)) \sqrt{2} (1 + (h^2 k^2)) \hat{C}^2 \delta^4 h^4 |u_j|_1^2, \end{aligned}$$

where \hat{C} is the positive constant involved in (A.17). Now, using (35) and taking into account that hypothesis (H3), it holds

$$|ShR_{ex} - S_{ex}Rh| \leq C\delta^4 h^2, \tag{39}$$

where C is a positive constant independent of h, k and δ (only dependent on α).

The denominator in (37) can be rewritten as

$$\begin{aligned} |RhR_{ex}| &= |B_k(u_j, u_{j+1})| |B_k(u_j - \tilde{\Psi}_j^v, u_{j+1} - \tilde{\Psi}_{j+1}^v) + B_k(u_j, u_{j+1})| \\ &\geq \frac{1}{h} (-1 + O(h^2 k^2)) \left(|B_k(u_j - \tilde{\Psi}_j^v, u_{j+1} - \tilde{\Psi}_{j+1}^v)| - \frac{1}{h} (-1 + O(k^2 h^2)) \right) \\ &\geq \frac{1}{h} (1 + O(h^2 k^2)) \left(\frac{1}{h} (1 + O(k^2 h^2)) - \sqrt{2} (1 + (h^2 k^2)) \hat{C}^2 \delta^4 h^4 \frac{1}{h} (2 + O(h^2 k^2)) \right) \end{aligned}$$

Once it is assumed (H4), it holds $1 - 2\hat{C}^2 \delta^4 h^4 \geq \beta > 0$ and hence the expression between large parenthesis in the last term of the inequality written above is strictly positive and lower bounded by β . So, it holds

$$|RhR_{ex}| \geq \frac{C}{h^2}, \tag{40}$$

being C a positive constant independent of h, k , and δ (only dependent on α and β). Finally, inserting estimates (39) and (40) in (37), it holds the first inequality in (34), and using analogous arguments to those used in [18, Theorem 3.2], the second inequality in (34) is obtained. \square

6. Discrete Green’s function and discrete inf-sup condition

Once the discrete dispersion relation has been studied, it is possible now to deduce the discrete Green’s function associated with the discrete sub-problem with matrix L_h^v , defined in (19). To write this discrete Green’s function, it will be followed by analogous arguments to those used in [32] in the continuous case, and in [17, Section 3.2]. Analogously to the continuous case, the expression of the discrete Green’s function $G_h(x_j, x_l)$ will be written in terms of two discrete functions α_h and β_h as follows:

$$G_h(x_j, x_m) = \begin{cases} \frac{\alpha_h(x_j)\beta_h(x_m)}{\Delta_h} & \text{if } x_j \leq x_m, \\ \frac{\beta_h(x_j)\alpha_h(x_m)}{\Delta_h} & \text{if } x_j > x_m, \end{cases} \quad (41)$$

where Δ_h is a quantity, which is fixed to satisfy

$$R_h G_h(x_{m-1}, x_m) + 2S_h G_h(x_m, x_m) + R_h G_h(x_{m+1}, x_m) = \frac{1}{h} \quad (42)$$

In the case of α_h , any homogeneous solution of the discrete variational problem with matrix L_h^v is given by a linear combination of the Bloch-type waves

$$\alpha_h(x) = A \sum_{j=0}^n \tilde{\Psi}_j^v(x) \cos(jk'h) + B \sum_{j=0}^n \tilde{\Psi}_j^v(x) \sin(jk'h) \quad (43)$$

The vector given by the values of α_h at the mesh vertices should satisfy the first row of the matrix L_h^v , this is, $2S_h \alpha_h(x_1) + R_h \alpha_h(x_2) = 0$. Using the discrete dispersion relation (33), it is straightforward to check that the equation above is equivalent to satisfy $\alpha_h(x_0) = 0$, and hence $A = 0$ and B is any non-null constant.

The computation of β_h can be deduced analogously. Since it can be defined by

$$\beta_h(x) = C \left(\sum_{j=0}^n \tilde{\Psi}_j^v(x) \cos(jk'h) + D \sum_{j=0}^n \tilde{\Psi}_j^v(x) \sin(jk'h) \right), \quad (44)$$

with C a non-null constant, it should only be checked that the last row of the linear system involving L_h^v is satisfied. In this case, it must be verified that $R_h \beta_h(x_{n-1}) + (S_h - ik) \beta_h(x_n) = 0$, or equivalently,

$$R_h (\cos(k^0 h(n-1)) + D \sin(k^0 h(n-1))) + (S_h - ik) (\cos(k^0 h n) + D \sin(k^0 h n)) = 0.$$

A direct computation from the equation written above shows that

$$D = \frac{\sin(k^0)\cos(k^0)(R_h^2 \sin^2(k^0 h) - k^2) - ikR_h \sin(k^0 h)}{R_h^2 \sin(k' h) \cos^2(k' h) + k^2 \sin^2(k' h)}$$

Additionally, straightforward computations also show that if it is taken $B = 1$ in (43) and $C = 1$ in (44) then

$$R_h \alpha h(x_{m-1}) \beta h(x_m) + 2S_h \alpha h(x_m) \beta h(x_m) + R_h \beta h(x_{m+1}) \alpha h(x_m) = -R_h \sin(k^0 h).$$

Hence, to satisfy (42), it is chosen $\Delta_h = -R_h h \sin(k^0 h)$. It should be remarked that since $k > \varepsilon$ (H2) and $kh \leq \alpha < \pi$ (H3), estimate (34) leads to $k^0 h < \alpha + C\delta^4 h^3$ which is smaller than π for δ and h small enough. Besides, from (36) and the estimate (40) it is guaranteed that R_h is lower bounded by a positive constant far from being null. Consequently, the Green's function given by (41) is well-defined.

The most attractive feature of the Green's function is that it allows writing the inverse of the matrix L_h^v explicitly, or equivalently, to write in closed form the solution of the linear system

$L_h^v \tilde{u}^v = \tilde{f}^v$. Using (41) and taking into account that the PUFEM discrete functions u^v_h in V^v_h are determined by the vector \tilde{u}^v_h of its point-wise values, it holds

$$\tilde{u}^v_h(x_l) = [\tilde{u}^v_h]_l = h \sum_{j=1}^n G_h(x_l, x_j) [\tilde{f}^v]_j. \quad (45)$$

From the equation written above, it is immediate to deduce that the coefficients of the inverse matrix of L_h^v (in the case of being uniquely defined) are given by $[(\mathcal{L}_h^v)^{-1}]_{lj} = hG_h(x_l, x_j)$.

Lemma 6.1. *Under hypothesis (H1)-(H4), given the source data $f \in L^2(0,1)$, if $u^v_h \in V^v_h$ is a solution of the discrete variational problem (21) then*

$$\|u^v_h\|_1 \leq C \|f\|_0, \quad (46)$$

where C is a positive constant independent of h , k , and δ (depending only on α and β).

Proof. The proof is entirely analogous to those one shown in [17, Lemma 3]. The estimate (46) is obtained by using the equivalence of norms stated in Lemma 4.6. \square

Remark 6.2. *The computation of the discrete Green function follows an analogous procedure used to compute the continuous Green function, which is specific for one-dimensional problems. Hence, these arguments cannot be extended straightforwardly to higher dimensions. Hence, the use of the tensor structure of the discrete problem to derive some estimates on the discrete Green function in higher dimensions remains as an open problem.*

Since the explicit computation of the discrete Green’s function and its well-posedness for $h(k + \delta) \leq \alpha < 1$ can be read as the proof of existence of solution for the discrete problem (21), the following theorem guarantees the uniqueness of solution by means of the discrete *inf-sup* condition (see [6] for a detailed discussion).

Lemma 6.3. Under hypothesis (H1)-(H4), it holds the discrete *inf-sup* condition

$$\inf_{\tilde{V}^v} \sup_{\tilde{V}^v} \frac{|B_k(u_h, v_h) - iku_h(1)v_h^-(1)|}{|u_h|_1} \geq \frac{C}{k}, \quad (47)$$

where C is a positive constant independent of h, k , and δ (depending only on α).

Proof. The same kind of arguments used in [17, Appendix B] will be followed. Inequality (47) is equivalent to show that

$$\sup_{v_h \in \tilde{V}^{hv}} \frac{|B_k(u_h, v_h) - iku_h(1)v_h^-(1)|}{|v_h|_1} \geq \frac{C}{k} |u_h|_1 \quad \text{for all } u_h \in \tilde{V}_h$$

To prove the inequality written above, an arbitrary $u_h \in \tilde{V}^{hv}$ is fixed and $v_h = u_h + z_h$ is defined, being z_h the solution of the auxiliary problem

$$B_k(w_h, z_h) - ikw_h(1)z_h^-(1) = k^2hw_h, z_h \mathbf{i}_{L^2(0,1)} \quad \text{for all } w_h \in \tilde{V}^{hv}.$$

Since $k^2u_h \in L^2(0,1)$, this problem has at least a solution given by the application of the discrete Green’s function. The arguments used in [17, Appendix B] in combination with the equivalence of norms stated in Lemma 4.6 shows that

$$|z_h|_1 \leq Ck \|u_h'\|_{k'}$$

with C a positive constant independent of h, k , and δ . From the estimation (34) and the assumptions of the present lemma, it is immediate to check that k/k^0 is bounded independently of h, k , and δ and hence it holds

$$|z_h|_1 \leq Ck |u_h|_1. \quad (48)$$

Coming back to the numerator in the *inf-sup* condition and using the expression of $v_h = u_h + z_h$, it is satisfied

$$\begin{aligned} B_k(u_h, v_h) - iku_h(1)v_h^-(1) &= B_k(u_h, u_h + z_h) - iku_h(1)(u_h^-(1) + z_h^-(1)) \\ &= B_k(u_h, u_h) - ik|u_h(1)|^2 + B_k(u_h, z_h) - iku_h(1)z_h^-(1) \end{aligned}$$

$$= B_k(u_h, u_h) - ik|u_h(1)|^2 + k^2 h u_h, u_h \dot{1}_{L^2(0,1)} = |u_h|_1^2 - ik|u_h(1)|^2,$$

and so, using (48), $|v_h|_1 \leq (1 + Ck)|u_h|_1$. In consequence, it holds

$$\sup_{|v_h|_1} \frac{|B_k(u_h, v_h) - ik u_h(1) \bar{v}_h(1)|}{|v_h|_1} \geq \frac{|u_h|_1^2}{|v_h|_1} \geq \frac{|u_h|_1^2}{(1 + Ck)|u_h|_1} = \frac{|u_h|_1}{1 + Ck}$$

which leads to (47) since k is strictly positive lower bounded far from zero. □

Finally, combining the stability estimates for the sub-problems stated in V^{h^v} and V^{b_h} , it can be stated a stability result for the whole discrete problem stated in the PUFEM discrete space V_h .

Theorem 6.4. *Under hypothesis (H1)-(H4), there exists a unique solution $u_h \in V_h$ of the discrete PUFEM problem (7). Also, it holds the stability estimate*

$$|u_h|_1 \leq Ck f_{k_0}, \tag{49}$$

where C is a positive constant independent of h , k , and δ .

Proof. The existence and uniqueness result comes straightforwardly from the existence and uniqueness solution of both sub-problems (21) and (11) defined in V^{h^v} and V^{b_h} , respectively. Also, since $u_h = u^{v_h} + u^{b_h}$, estimate (49) is obtained combining (20) and (46). □

7. Robustness analysis of the PUFEM approximation

Finally, this section is devoted to writing an error estimate for the PUFEM discretization. More precisely, the H^1 -distance between oscillatory functions, which are exact solutions of the Helmholtz problem, and the PUFEM approximations will be estimated. The main three ingredients to obtain such estimates are the stability of the discrete PUFEM variational problem (stated in the previous section), the interpolant estimates for oscillatory solutions described in Appendix A, and its relation with the projections of the exact solution in the PUFEM discrete space.

Firstly, to highlight the difficulties of passing to the limit when $h(k + \delta)$ tends to zero, it will be shown that the functions belonging to the PUFEM space on uniform meshes satisfy an inverse inequality, once the limit case $h(k + \delta) = 0$ is avoided.

Lemma 7.1 (Inverse inequality). *Under hypothesis (H3) and (H5), there exist constants C_0 and C_1 independent of h , k and δ (only dependent on ε and α) such that*

$$C_0 \qquad C_1$$

$$\frac{1}{h} \|k v_h\|_0 \leq |v_h|_1 \leq \frac{1}{h} \|k v_h\|_0, \tag{50}$$

for all $v_h \in V_h$.

Proof. A slight modification of the steps used in [8, Chapter 3] will be followed to proof the classical inverse inequality in standard polynomial spaces, for instance, for any continuous piecewise P^1 -discrete function $v_h^{fe} \in \langle \{\Phi_j\}_{j=0}^n \rangle$ defined on a one-dimensional equispaced mesh, where it is satisfied $|v_h^{fe}|_1 \leq C/h \|v_h^{fe}\|_0$.

Direct inspection reveals that all these shape functions depend continuously on the parameter $h(k + \delta) \in [\varepsilon, \alpha]$. In addition, if K_{loc} and M_{loc} denote the local stiffness and mass matrices with respect to this local shape basis, the coefficients of these matrices also depend continuously on the parameter $h(k + \delta)$, and it holds

$$\lambda_{\min}(h(k + \delta)) \leq \frac{\tilde{v}^* K_{loc} \tilde{v}}{\tilde{v}^* M_{loc} \tilde{v}} \leq \lambda_{\max}(h(k + \delta)),$$

where $\lambda_{\min}(h(k + \delta))$ and $\lambda_{\max}(h(k + \delta))$ are respectively the minimum and maximum eigenvalues of the symmetric generalized eigenvalue problem $K_{loc} \tilde{v} = \lambda M_{loc} \tilde{v}$, whose eigensolutions also depend continuously on the parameter $h(k + \delta)$. Hence, the maps $h(k + \delta) \mapsto \lambda_{\min}(h(k + \delta))$ and $h(k + \delta) \mapsto \lambda_{\max}(h(k + \delta))$ are continuous functions defined in a non-empty compact domain $[\varepsilon, \alpha]$. So, using the Weierstrass theorem, both continuous functions reach respectively a minimum λ_{\min} and a maximum value λ_{\max} (possibly depending on ε and α). Hence, taking into account that $|\hat{v}_j|_{H^1(\hat{T})}^2 = \tilde{v}^* K_{loc} \tilde{v}$ and $\|\hat{v}_j\|_{L^2(\hat{T})}^2 = \tilde{v}^* M_{loc} \tilde{v}$, it holds

$$\lambda_{\min} \|\hat{v}_j\|_{L^2(\hat{T})}^2 \leq |\hat{v}_j|_{H^1(\hat{T})}^2 \leq \lambda_{\max} \|\hat{v}_j\|_{L^2(\hat{T})}^2,$$

or equivalently, coming back to the element T_j ,

$$\lambda_{\min} \|v_h|_{T_j}\|_{L^2(T_j)}^2 \leq |v_h|_{T_j}|_{H^1(T_j)}^2 \leq \lambda_{\max} \|v_h|_{T_j}\|_{L^2(T_j)}^2 \quad \begin{matrix} 1 \\ \text{for } j \\ = 0, \dots, n. \end{matrix} \quad \begin{matrix} h \\ h \end{matrix}$$

If the terms from $j = 0$ to n in the previous inequality are added and the root square is computed, estimates (50) are obtained. \square

Remark 7.2. Assumption (H5) implies $\varepsilon < h(k + \delta)$, which is essential to avoid the limit case $h(k + \delta) = 0$. However, it does not mean any restriction on the error analysis, since ε can be chosen as small as desired independently of k and δ . As it has been discussed previously at the beginning of Section 4, if the limit case $h(k + \delta) = 0$ is formally considered, the PUFEM subspace V_h will be identical to the standard continuous piecewise P^1 -finite element space and the restrictions of functions of V_h^b at each element

coincide with the P^2 -bubble functions. In the classical polynomial bubble space, the number of bubbles coincides with the number of elements, i.e., n . However, the number of basis elements in V_h^b coincides with the number of vertices $n+1$. So, in the limit case of $h(k+\delta) = 0$, the twin-bubble basis of V_h^b collapses and a function of this discrete basis should be removed to avoid a linear dependency.

Finally, an *a priori* error estimate for the approximation computed by means of the PUFEM discretization can be obtained.

Theorem 7.3. *Let $u \in H^1(0,1)$ be a solution of the variational problem (2) and let $u_h \in V_h$ be the solution of the PUFEM discrete problem defined in (7), both with null source term $f = 0$. Under assumptions (H1)-(H5), it holds*

$$|u - u_h|_1 \leq Ck |u - I_h u|_1, \quad (51)$$

where C is a positive constant independent of h , δ , and k .

Proof. Firstly, since $u - u_h$ is orthogonal to V_h with respect to the sesquilinear form of the variational problem (7), it holds

$$B_k(u - u_h, v_h) - ik(u(1) - u_h(1))\bar{v}_h(1) = 0,$$

for all $v_h \in V_h$. Hence, if $z_h = u_h - I_h u \in V_h$ then, since $z_h = (u_h - u) + (u - I_h u)$, the discrete function z_h is the solution of the following variational problem:

$$B_k(z_h, v_h) - ikz_h(1)\bar{v}_h(1) = B_k(u - I_h u, v_h),$$

for all $v_h \in V_h$. Since $V_h = \tilde{V}_h^v \oplus V_h^b$, the variational equality written above is satisfied independently for test functions in the vertex-value space \tilde{V}_h^v and the twin-bubble space V_h^b . The same kind of considerations can be applied to split z_h , this is, $z_h = z_h^v + z_h^b$. Due to the orthogonality relation between the discrete spaces \tilde{V}_h^v and V_h^b , each of these functions, z_h^v and z_h^b are respectively solution of the variational problems

$$B_k(z_h^v, v_h^v) - ikz_h^v(1)\bar{v}_h^v(1) = B_k(u - I_h u, v_h^v) \quad \text{for all } v_h^v \in \tilde{V}_h^v,$$

$$B_k(z_h^b, v_h^b) = B_k(u - I_h u, v_h^b) \quad \text{for all } v_h^b \in V_h^b.$$

Also, due to the linearity of these two problems, their solutions can be rewritten as the sum of two new discrete functions, $z_h^v = z_{1h}^v + z_{2h}^v$ and $z_h^b = z_{1h}^b + z_{2h}^b$, where each addend is solution respectively of the following variational problems:

$$B_k(z_{1h}^v, v_h^v) - ikz_{1h}^v(1)\bar{v}_h^v(1) = \langle (u - I_h u)', (v_h^v)' \rangle_{L^2(0,1)} \quad \text{for all } v_h^v \in \tilde{V}_h^v, \quad (52)$$

$$B_k(z_{2h}^v, v_h^v) - ikz_{2h}^v(1)\bar{v}_h^v(1) = -k^2 \langle u - I_h u, v_h^v \rangle_{L^2(0,1)} \quad \text{for all } v_h^v \in \tilde{V}_h^v, \quad (53)$$

$$B_k(z_{1h}^b, v_h^b) = \langle (u - I_h u)', (v_h^b)' \rangle_{L^2(0,1)} \quad \text{for all } v_h^b \in V_h^b, \quad (54)$$

$$B_k(z_{2h}^b, v_h^b) = -k^2 \langle u - I_h u, v_h^b \rangle_{L^2(0,1)} \quad \text{for all } v_h^b \in V_{bh}. \quad (55)$$

For each one of the solutions of the discrete variational problems stated above, some of the estimates written in the previous sections can be applied. More precisely, if analogous derivations to those used to obtain (48), a coercive estimate similar to (12), and (15) are applied respectively to the solutions of problems (52)-(55), then it is satisfied

$$\begin{aligned} |z_{1h}^v|_1 &\leq Ck|u - I_h u|_1, \\ |z_{2h}^v|_1 &\leq Ck \left| \frac{k}{k'} \right| |u - I_h u|_1, \\ |z_{1h}^b|_1 &\leq C|u - I_h u|_1, \\ |z_{2h}^b|_1 &\leq Chk^2|u - I_h u|_1, \end{aligned}$$

where C is a positive constant independent of h , k , and δ (depending only on α and β).

Finally, collecting all these estimates and using the fact that $z_h = z_{1h}^v + z_{2h}^v + z_{1h}^b + z_{2h}^b$, then

$$|z_h|_1 \leq C(1+k)|u - I_h u|_1 + Ck|u - I_h u|_1,$$

from which (51) is concluded applying a Poincaré inequality and due to k is strictly positive lower bounded far from zero. \square

Remark 7.4. The arguments used in this section are not specific for the one-dimensional case and they can be used in the numerical analysis of the problem in higher dimensions, once the interpolant operator I_h has been designed in a similar manner (see Remarks A.3-A.5).

Corollary 7.5. *Let $u \in H^1(0,1)$ be an oscillatory solution of the variational problem (2) and let $u_h \in V_h$ be the solution of the PUFEM discrete problem defined in (7), both with null source term $f = 0$. Under assumptions (H1)-(H5), it holds*

$$|u - u_h|_1 \leq Ckh^2\delta^2|u|_1, \quad (56)$$

where C is a positive constant independent of h , δ , and k .

Proof. The combination of estimates (51) and (A.17) leads to (56). \square

As it will be checked in the following section, this estimate can be improved for oscillatory solutions. Since they are solutions of the Helmholtz equation with smooth right-hand side $f \in H^l(0,1)$ with $l \geq 1$, duality stability estimates (analogous to that one described in [18, Theorem 3.2]) should be used to obtain a more accurate estimate (possibly independent of k).

8. Numerical Results

In this section, some numerical results are shown in order to illustrate how the PUFEM discrete errors depend on the mesh size h , the wave number k , and the perturbation parameter δ . For this purpose, the boundary data are chosen in problem (1) to obtain $u(x) = \sin(kx)$ as the exact solution. Firstly, plots in Figure 1 illustrate the second-order accuracy of the PUFEM interpolation errors

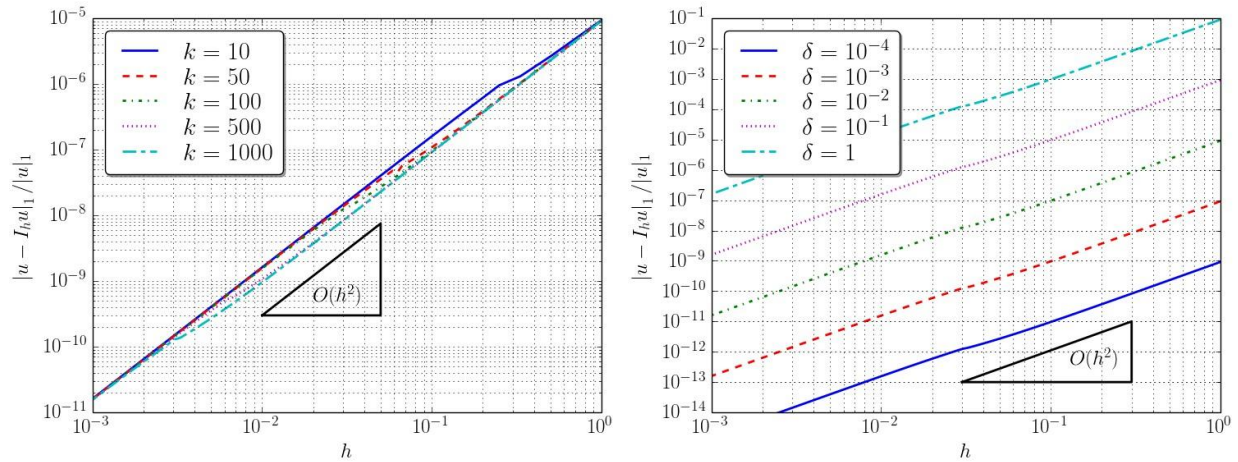


Figure 1: Interpolation H^1 -errors of the PUFEM solution (computed when the exact solution is given by $u(x) = \sin(kx)$), plotted with respect to the mesh size but fixing the value of the perturbation parameter $\delta = 10^{-2}$ (left) or the wave number $k = 100$ (right).

with respect to the mesh size h and the spurious perturbation parameter δ . It can be observed that the error estimates obtained in Appendix A are sharp in terms of both parameters h and δ , and independent of the wave number value.

The relative error for the PUFEM discretization has been computed in terms of the H^1 -seminorm. All the computations have been performed with 48 digits of precision using the ADVANPIX toolbox [22], to avoid round-off errors and numerical instabilities coming from a high condition number associated with the matrices involved in the discrete PUFEM linear systems. Besides, the H^1 relative errors have been computed using the approximation $|u - u_h|_1 \approx (\tilde{u}_h - I^h u)^* K_h (\tilde{u}_h - I^h u)$, where \tilde{u}_h is the vector of degrees of freedom corresponding to the PUFEM approximation u_h , K_h is the discrete stiffness matrix associated to the PUFEM method, and $\tilde{I}^h u$ is the vector of degrees of freedom corresponding to the PUFEM interpolation function $I_h u$ of the exact solution u .

Plots in Figure 2 illustrate the second-order accuracy of the PUFEM approximation with respect to the mesh size h and the spurious perturbation parameter δ . Moreover, Figure 2 also shows the dependence of PUFEM relative errors on the wave number k . It can be checked that the overall trend exhibited by the PUFEM relative error does not depend on the wave number value. However, the position of the first peak in the error curves depends on the wave number (moving to lower values of h as soon as k is

increased). Also, the convergent second-order behavior of the perturbation parameter δ that holds in (51) for the PUFEM discretization can be checked for H^1 -error curves.

Finally, the estimated 1-norm condition number [12] associated with the PUFEM discrete matrix is shown in Figure 3. Two different behaviors are observed at pre-asymptotic ($hk \ll 1$) and

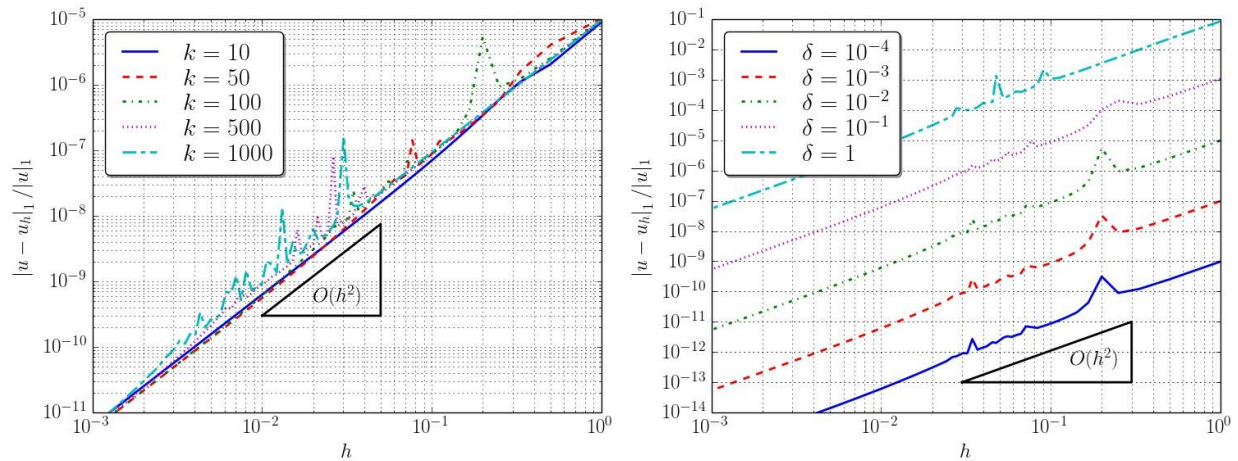


Figure 2: Approximation H^1 -errors of the PUFEM solution (computed when the exact solution is given by $u(x) = \sin(kx)$), plotted with respect to the mesh size but fixing the value of the perturbation parameter $\delta = 10^{-2}$ (left) or the wave number $k = 100$ (right).

asymptotic regime ($hk \gg 1$) of order h^{-1} and h^{-6} , respectively. It can also be checked that the peaks on the condition number correspond to the peaks, also presented in the approximation H^1 errors reported in Figure 2.

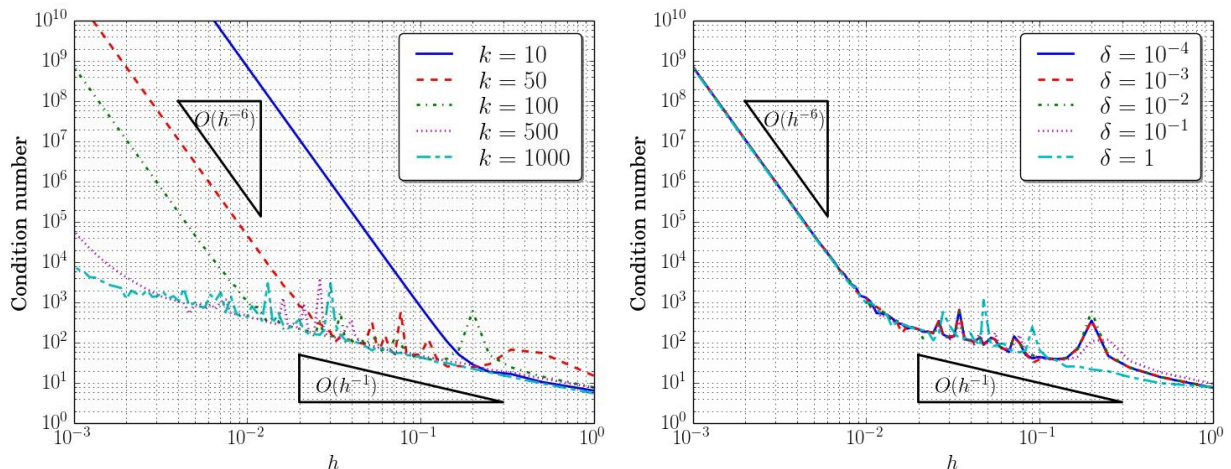


Figure 3: Condition number of the PUFEM discrete matrix plotted with respect to the mesh size but fixing the value of the perturbation parameter $\delta = 10^{-2}$ (left) or the wave number $k = 100$ (right).

9. Analysis extension to higher dimensions

The starting point for the pollution and numerical dispersion analysis of any kind of numerical method in higher dimensions consists in the study of their numerical properties in a onedimensional problem. Examples of such process can be found for instance in [13] and [1], where the one-dimensional FEM problem is used as a stepping stone to analyze the two- or threedimensional case in uniform structured meshes (or tensor product meshes). The case of the PUFEM method is not an exception, and the present contribution represents the first effort on performing such one-dimensional analysis in the scientific literature.

The present work has two novel main ingredients in the PUFEM numerical analysis: (i) the use of a global condensation procedure to split the discrete space between nodal-supported functions and those others, which can be understood as “bubble”-like discrete functions, (ii) the use of specific wave-like interpolation operator to obtain a plane-wave representation of smooth solutions. Beyond the specificities of the one-dimensional computations, these two key ingredients should be present in the dispersion analysis in higher dimensions.

10. Conclusions

In this work, a one-dimensional Helmholtz problem and its weak formulation have been considered. The *inf-sup* continuous and discrete conditions have been demonstrated. A plane wave based PUFEM discretization in terms of exponential and trigonometrical functions has been described. Two interpolation estimates have been proved, and from that, an *a priori* error estimate for the approximation computed by means of the PUFEM discretization has been deduced. The numerical results confirm the second order of accuracy of the PUFEM approximation with respect to the mesh size h and the additional perturbation parameter δ that is stated in the error estimate. However, the error estimates obtained are not optimal with respect to the wave number parameter. To obtain sharper estimates in terms of the wave number requires a finer analysis on the spectrum of the PUFEM discrete matrix (and subsequently, also on its condition number), which is not included in the scope of the present work and it will be part of the topics of further research.

Additionally, it should be mentioned that the robustness and the numerical dispersion analysis presented in this work are applicable to the numerical analysis of a domain decomposition method [2] focused on the solution of vibrational problems in three-dimensional trusses structures [30], which are forced to work in tension/compression. This three-dimensional application is far from the scope of the present article and it will be part of a forthcoming work.

Acknowledgements

This work has been supported by Xunta de Galicia project “Numerical simulation of highfrequency hydro-acoustic problems in coastal environments - SIMNUMAR”

(EM2013/052), cofunded with European Regional Development Funds (ERDF). Moreover, the first and third authors have been supported by MINECO grants MTM2014-52876-R and MTM2017-82724-R, and the second author has been supported by Junta de Castilla y Leon under project VAO24P17, co-financed by ERDF funds.

Appendix A. Interpolation estimates

The design of an accurate interpolant-like operator for PUFEM involves two strategies, which are going to be combined in order to obtain an accurate and computational efficient discrete approximation of a given function. First, an interpolant-like operator will be defined for any mesh size h , which will be qualified as pre-asymptotic. Second, for h small enough, a P_2 -based interpolant will be recast for the PUFEM discrete space, which will be identified as an asymptotic interpolant. Finally, the combination of both approximations allows an accurate approximation for the H^1 -projection in the PUFEM discrete space.

Appendix A.1. Pre-asymptotic interpolant-like operator

Any given function $v \in H^2(0,1)$ has been split into two parts, traveling, respectively, to the right (and whose intensity vector points towards the positive axis) and to the left. This splitting is given by the differential operators involved in the Sommerfeld radiation condition, this is, for $v \in C^1(0,1)$,

$$\frac{1}{2ik} (v' + ikv) - \frac{1}{2ik} (v' - ikv) \quad v = \quad (A.1)$$

| {z } | {z } right-traveling left-traveling

Then, the interpolant $I_p v \in X_h$ is defined by

$$I_p v = \frac{1}{2ik} \sum_{j=0}^n \left((v'(x_j) + ikv(x_j)) \psi_j^+ - (v'(x_j) - ikv(x_j)) \psi_j^- \right) \quad (A.2)$$

From (A.2) and (8), it is immediate to check that

$$(I_p v)(x) = \sum_{j=0}^n \left(\frac{v'(x_j)}{k} \psi_j^b(x) + v(x_j) \psi_j^v(x) \right) \quad (A.3)$$

and hence, it holds $I_p v(x_j) = v(x_j)$ trivially.

However, despite of having used the point-wise values of the derivatives at the mesh nodes $v'(x_j)$, $(I_p v)'(x_j) \neq v'(x_j)$ and, moreover, $I_p v$ does not belong to $C^1(0,1)$. So, the point-wise evaluation of the derivative of $I_p v$ is not well-defined.

An unusual feature of the interpolant-like operator $I_p : H^2(0,1) \rightarrow X_h$ is that, in general, $I_p v_h \neq v_h$ for a given $v_h \in X_h$, as it can be shown considering $v_h(x) = e^{i(k+\delta)x}$. In this case, for $\delta \neq 0$, and taking into account (A.2),

$$v_h = \sum_{j=0}^n e^{i(k+\delta)x_j} \psi_j^+ \neq \sum_{j=0}^n \left(\left(1 + \frac{\delta}{2k} \right) e^{i(k+\delta)x_j} \psi_j^+ - \frac{\delta}{2k} e^{i(k+\delta)x_j} \psi_j^- \right) = I_p v_h.$$

However, it is fulfilled that $I_p(X_h) \subseteq X_h$, $I_p(V_h) \subseteq V_h$, and also the following error estimate:

Lemma A.1. *Under hypothesis (H1)-(H2), if $u \in V$ is a solution of the homogeneous Helmholtz equation, then there exists the interpolant-like discrete function $u_I = I_p u \in X_h$ defined by (A.2) that satisfies*

$$\begin{aligned} |u - v_h|_1 &\leq |u - I_p u|_1 \leq \left(\frac{Ch}{k} + \hat{C}h^2 \right) \delta^2 | \inf_{v_h \in X_h} \|ku - v_h\|_0 \leq \|ku - I_p u\|_0 \leq Ch^2 \delta^2 \|ku\|_0, \end{aligned} \tag{A.4}$$

$$\inf_{v_h \in X_h} \|u - v_h\|_1, \tag{A.5}$$

where the positive constants C and \hat{C} only depend on ϵ .

Proof. Firstly, since u is the solution of the Helmholtz equation with null right-hand side, $u \in H^2(0,1)$, and so $I_p u$ is well-defined. Now, since $u_I = I_p u \in X_h$, any restriction of u_I to the mesh element $[x_j, x_{j+1}]$ should be written as a linear combination of basis functions in X_h which are not null on that element, this is, those functions multiplied by ϕ_j and ϕ_{j+1} . Hence, if $x \in [x_j, x_{j+1}]$,

$$\begin{aligned} u_I(x) &= \alpha_{1j} \psi^+_j(x) + \alpha_{2j} \psi^+_{j+1}(x) + \alpha_{3j} \psi^-_j(x) + \alpha_{4j} \psi^-_{j+1}(x) \\ &= \alpha_{1j} \phi_j(x) e^{i(k+\delta)(x-x_j)} + \alpha_{2j} \phi_{j+1}(x) e^{i(k+\delta)(x-x_{j+1})} \\ &\quad + \alpha_{3j} \phi_j(x) e^{-i(k+\delta)(x-x_j)} + \alpha_{4j} \phi_{j+1}(x) e^{-i(k+\delta)(x-x_{j+1})}, \end{aligned} \quad \text{for } x \in [x_j, x_{j+1}].$$

Since the exact solution for the homogeneous Helmholtz equation is given by $u(x) = Ae^{ikx} + Be^{-ikx}$, from (A.2) it is easy to check that $\alpha_{1j} = Ae^{ikx_j}$, $\alpha_{2j} = Ae^{ikx_{j+1}}$, $\alpha_{3j} = Be^{-ikx_j}$ and $\alpha_{4j} = Be^{-ikx_{j+1}}$ for $j = 0, \dots, n$, and so it holds

$$\|u - u_I\|_0^2 \leq (|A|^2 + |B|^2) \sum_{j=0}^{n-1} \int_{x_j}^{x_{j+1}} \left| e^{ikx} - e^{-i\delta x_j} \phi_j(x) e^{i(k+\delta)x} - e^{-i\delta x_{j+1}} \phi_{j+1}(x) e^{i(k+\delta)x} \right|^2 dx.$$

The integrals in the previous sum can be computed explicitly, and it is immediate to check that they are identical (the integrands are the square modulus of conjugate expressions) and independent of the mesh element $[x_j, x_{j+1}]$, and the wave number k . For the trivial case ($\delta = 0$), it is direct to prove that their value is null. For $\delta \neq 0$, it holds

$$\int_{x_j}^{x_{j+1}} \left| e^{ikx} - e^{-i\delta x_j} \varphi_j(x) e^{i(k+\delta)x} - e^{-i\delta x_{j+1}} \varphi_{j+1}(x) e^{i(k+\delta)x} \right|^2 dx$$

$$= \int_0^h \left| 1 - \frac{h-x}{h} e^{i\delta x} - \frac{x}{h} e^{i\delta(x-h)} \right|^2 dx = \frac{5}{3}h - \frac{4}{\delta^2 h} + \left(\frac{h}{3} + \frac{4}{\delta^2 h} \right) \cos(\delta h),$$

and taking into account the identical contribution of the integrals in each element of the mesh,

$$\|u - u_1\|_0^2 \leq (|A|^2 + |B|^2) \frac{1}{h} \left(\frac{5}{3}h - \frac{4}{\delta^2 h} + \left(\frac{h}{3} + \frac{4}{\delta^2 h} \right) \cos(\delta h) \right).$$

Now, using a Taylor expansion for the expression in the second term of the previous inequality and (A.8), it holds

$$\|u - u_1\|_0^2 \leq (|A|^2 + |B|^2) \frac{17}{360} \delta^4 h^4 \leq \frac{17C_\epsilon}{360} \delta^4 h^4 \|u\|_0^2, \tag{A.6}$$

and so (A.4) is proved.

In order to obtain (A.5), analogous arguments can be utilized to bound the H^1 -seminorm of $u - u_1$. In fact, for $\delta \neq 0$, using straightforward computations on the integral contribution at each mesh element and taking into account a Taylor expansion for the h -dependent expressions, it holds

$$\|u - u_1\|_1^2 \leq (|A|^2 + |B|^2) \sum_{j=0}^n \left(\frac{h}{4k^2} + hk^2 + \frac{h(k + |\delta|)^2}{\delta^2 h} - 2(k + |\delta|) \sin(|\delta| h) + 2 \cos(\delta h) \left(-\frac{1}{h} + \frac{h}{6}(k + |\delta|)^2 + \frac{2k^2}{\delta^2 h} \right) \right) \leq \frac{C_\epsilon}{12} \delta^4 \frac{h^2}{k^2} \|u\|_1^2 + \frac{7C_\epsilon}{72} \delta^4 h^4 \|u\|_1^2. \tag{A.7}$$

In the last inequality written above, it has been used that $|\delta|/k \leq 1$ (assumption (H1)), and an analogous estimate to (A.8) for the H^1 -seminorm, this is, $k^2(|A|^2 + |B|^2) \leq C_\epsilon \|u\|_1^2$. Hence, estimate

(A.5) is obtained, with positive constants $C = C_\epsilon/12$ and $C^* = 7C_\epsilon/72$ independent of h , δ , and k . \square

Remark A.2. To obtain (A.6), it has been used

$$|A|^2 + |B|^2 \leq C_\varepsilon \|u\|_0^2, \quad (\text{A.8})$$

with $C_\varepsilon > 0$ depending only on ε . This bound can be derived immediately since the exact solution is given by $u(x) = Ae^{ikx} + Be^{-ikx}$ and so

$$\begin{aligned} \|u\|_0^2 &= \int_0^1 |Ae^{ikx} + Be^{-ikx}|^2 dx = \int_0^1 \left(|A|^2 + |B|^2 + 2\operatorname{Re}(A\bar{B}e^{2kix}) \right) dx \\ &= |A|^2 + |B|^2 - \frac{\operatorname{Re}(A\bar{B})}{k} \sin(2k) - \frac{\operatorname{Im}(A\bar{B})}{k} \cos(2k) \\ &\geq |A|^2 + |B|^2 - \frac{2}{k} |A||B| \geq \left(1 - \frac{1}{k}\right) (|A|^2 + |B|^2) \geq \left(1 - \frac{1}{\varepsilon}\right) (|A|^2 + |B|^2), \end{aligned}$$

where assumption (H2) ensures that $1 - 1/k$ is a monotonically decreasing function, bounded in $[\varepsilon, +\infty)$, and so satisfying the estimate (A.8) with $C_\varepsilon = 1 - 1/\varepsilon$.

Remark A.3. The pre-asymptotic interpolation procedure introduced above is based on a planewave representation of the solutions of the Helmholtz problem. So, its extension to higher dimensions this kind of novel interpolants should be extended based on the Vekua's theory [28]. More precisely, in the two-dimensional case, assuming that the preferred angles of incidence θ_l , $l = 0, \dots, M$, are uniformly distributed in $(0, 2\pi]$ (see Remark 3.1), and M is odd, then any smooth function v could be split into $M + 1$ -terms as follows:

$$v = \sum_{l=0}^M \left(\nabla v \cdot \frac{\vec{k}_l}{k} + ikv \right) e^{i\vec{k}_l \cdot \vec{x}}$$

with $\vec{k}_l = k(\cos \theta_l, \sin \theta_l)^T$, $l = 0, \dots, M$. Hence, in the two-dimensional case the interpolant $I_p v \in X_h$ is given by

$$[I_p(v)](\vec{x}) = \frac{1}{(M+1)ik} \sum_{j=0}^n \sum_{l=0}^M \left(\nabla v \cdot \frac{\vec{k}_l}{k} + ikv(\vec{x}_j) \right) e^{i\vec{k}_l \cdot \vec{x}} \Phi_j(\vec{x}),$$

where \vec{x}_j , $j = 0, \dots, n$, are the coordinates of the vertices in the mesh.

Appendix A.2. Asymptotic P_2 -based interpolant

In this subsection, an asymptotic interpolant I_2 is introduced when the product $h(k + |\delta|)$ is bounded (which holds under hypothesis (H3)). The definition is based on the standard P_2 interpolant. Then, for a given $v \in H^1(0,1)$, the interpolant $I_2 v(x) = \sum_{j=0}^n (\gamma_j^b \psi_j^b(x) + \gamma_j^v \psi_j^v(x)) \in X_h$ is defined by imposing

$$I_2 v(x_j) = v(x_j) \quad \text{for } j = 0, \dots, n, \tag{A.9}$$

$$I_2^2 v \left(\frac{x_j + x_{j+1}}{2} \right) = \left(\frac{x_j + x_{j+1}}{2} \right) v \quad \text{for } j = 0, \dots, n-1. \tag{A.10}$$

Since these conditions form a set of $2n+1$ linear equations, an additional equation is required to have a well-posed linear problem with a unique solution (see Remark 7.2 for a detailed discussion). Arbitrarily, it can be fixed $\gamma_0^b = 0$. From (A.9), $\gamma_j^v = v(x_j)$. So, since $\gamma_0^b = 0$, it is necessary to compute only γ_j^b for $j = 1, \dots, n-1$. Then, taking into account (A.10) for $j = 1, \dots, n$,

$$v \left(\frac{x_j + x_{j+1}}{2} \right) = \gamma_j^b \phi_j \left(\frac{x_j + x_{j+1}}{2} \right) \sin \left((k + \delta) \frac{h}{2} \right) - \gamma_{j+1}^b \phi_{j+1} \left(\frac{x_j + x_{j+1}}{2} \right) \sin \left((k + \delta) \frac{h}{2} \right),$$

which leads to

$$\gamma_{j+1}^b = \frac{-2}{\sin \left((k + \delta) \frac{h}{2} \right)} \left(v \left(\frac{x_j + x_{j+1}}{2} \right) - \frac{\gamma_j^b}{2} \sin \left((k + \delta) \frac{h}{2} \right) \right) \quad \text{for } j = 1, \dots, n$$

Notice that, since $h(k+\delta) < \pi$, then the expression $\sin((k+\delta)h/2)$ will always be strictly positive, and the coefficients γ_j^b for $j = 0, \dots, n$ are always well-defined.

Lemma A.4. *If $v \in V$ is a solution of the homogeneous Helmholtz equation, then there exists a constant C independent of h, k and δ such that*

$$\|v - I_2 v\|_0 \leq Ch^3 k^3 \|v\|_0, \tag{A.11}$$

$$\|v - I_2 v\|_1 \leq Ch^2 k^2 \|v\|_1. \tag{A.12}$$

Proof. Let I_{P_2} be the continuous piecewise P^2 interpolant. Since v is a solution of the homogeneous Helmholtz equation, $v \in H^3(0,1)$ and hence, the order of approximation of this polynomial interpolant is optimal in the sense that (see [18, Section 1.5])

$$\|v - I_{P_2} v\|_0 + h \|v - I_{P_2} v\|_1 \leq Ch^3 \|v\|_3, \tag{A.13}$$

where C is a constant independent of h . Direct computations, analogous to those used in Lemma A.1 (taking into account that v is a linear combination of sine and cosine functions

and using the Taylor approximations of the PUFEM local basis functions) allow us to prove

$$\|v - I_2 v\|_0 + h \|v - I_2\|_1 \leq Ch^3 |v|_3,$$

from which (A.11) and (A.12) follows by using that v is an oscillatory solution (and hence $|v|_3 \leq Ck^3 \|v\|_0$ and $|v|_3 \leq Ck^2 |v|_1$, being C a positive constant independent of k). \square

Remark A.5. An analogous argument can be extended to higher dimensions to define an adequate asymptotic polynomial interpolant. In the case of a PUFEM enrichment involving $M + 1$ plane waves (see Remark 3.1), then I_2 should be replaced by a P^m -based interpolant with $m \geq 2$, where m depends on M , and it must be selected to match the order of convergence of the pre-asymptotic interpolant I_p .

Appendix A.3. An accurate global interpolation procedure

Finally, the combination of the pre-asymptotic interpolant-like operator I_p and the asymptotic interpolant I_2 , leads to an accurate global interpolant I_h , with similar approximation properties to those exhibited by the discrete projection operators. This new global operator $I_h: H^1(0,1) \rightarrow X_h$ is given by $I_h v = I_p v$ if $h(k + |\delta|) \geq \pi$ (pre-asymptotic regime) and $I_h v = I_p v + I_2 v - I_2 I_p v$ if $h(k + |\delta|) < 1$ (asymptotic regime under hypothesis (H3)). Due to the approximation properties of both interpolant operators, it is easy to obtain estimates for this new operator I_h as follows.

Lemma A.6. Under hypothesis (H1)-(H2), if $u \in V$ is a solution of the homogeneous Helmholtz equation, then it holds: if $h(k + |\delta|) > \pi$,

$$\|ku - I_h u\|_0 \leq Ch^2 \delta^2 \|ku\|_0, \quad (\text{A.14})$$

$$|u - I_h u|_1 \leq Ch^2 \delta^2 |u|_1, \quad (\text{A.15})$$

and, if $h(k + |\delta|) < 1$ (hypothesis (H3)),

$$\|ku - I_h u\|_0 \leq Ch^3 k \delta^2 \|ku\|_0, \quad (\text{A.16})$$

$$|u - I_h u|_1 \leq Ch^2 \delta^2 |u|_1, \quad (\text{A.17})$$

where the positive constants C and \hat{C} do not depend on h , k , and δ .

Proof. First, the case $hk \geq \pi$ is considered. In this case, $I_h = I_p$, which gives directly (A.14) from (A.4). Estimate (A.15) follows from (A.5), since, for $hk \geq \pi$,

$$|u - I_h u|_1 \leq \left(\frac{Ch}{k} + \hat{C}h^2 \right) \leq (C + \hat{C})h^2 \delta^2 |u|_1.$$

Then, the case $h(k + |\delta|) < 1$ is considered. Using the fact that $2\pi/k$ is an upper bound of the mesh size h , (A.4) implies

$$\|u - I_p\|_0 \leq Ch^2\delta^2\|u\|_0 \leq \frac{C\delta}{2} \|u\|_0 \quad \text{---} \\ \text{. (A.18)} \\ k$$

Then, $\|u - I_h u\|_0 = \|u - (I_p u + I_2 u - I_2 I_p u)\|_0 = \|(u - I_p u) - I_2(u - I_p u)\|_0$ taking into account the definition of the operator I_h and estimates (A.11) and (A.18),

$$\leq Ch^3 k^3 \|u - I_p u\|_0 \leq Ch^3 k^3 \frac{C\delta}{2} \|u\|_0 = C^2 h^3 k \delta^2 \|u\|_0 \\ \text{---} , k$$

and hence (A.16) is obtained. Analogously, from (A.5) and since $h \leq 2\pi/k$,

$$\|u - I_p\|_1 \leq Ch^2\delta^2|u|_1 \leq \frac{C\delta}{2} |u|_1 \quad \text{---} \\ \text{. (A.19)} \\ k$$

Then, $|u - I_h u|_1 = |u - (I_p u + I_2 u - I_2 I_p u)|_1 = |(u - I_p u) - I_2(u - I_p u)|_1$ taking into account the definition of the operator I_h and estimates (A.12), and (A.19),

$$\leq Ch^2 k^2 |u - I_p u|_1 \leq Ch^2 k^2 \frac{C\delta}{2} |u|_1 = C^2 h^2 \delta^2 |u|_1 \\ \text{---} , k$$

and consequently (A.17) follows. \square

Remark A.7. In view of the arguments used in the proof described above, the operator I_h can be read as a correction of the interpolant-like operator I_p using the I_2 -interpolant of its approximation error. More precisely, if e_h denotes the interpolation error made by $I_p u$ (i.e., $e_h = u - I_p u$) then the value of the global interpolation under hypothesis (H3), this is, for $h(k + |\delta|) < 1$, is given by $I_h u = I_p u + I_2 e_h$. Hence, it is shown that I_h is an interpolant operator in V_h at the mesh vertices $\{x_j\}_{j=0}^n$ since

$$(I_h u)(x_j) = (I_p u)(x_j) + (I_2 e_h)(x_j) = (I_p u)(x_j) + e_h(x_j) = u(x_j).$$

References

- [1] M. Ainsworth. Discrete dispersion relation for hp-version finite element approximation at high wave number. *SIAM Journal on Numerical Analysis*, 42(2):553–575, 2004.

- [2] Jean-David Benamou and Bruno Despres. A domain decomposition method for the helmholtz equation and related optimal control problems. *Journal of Computational Physics*, 136(1):68–82, 1997.
- [3] A. Bermudez, D. Gómez, and P. Salgado. *Mathematical Models and Numerical Simulation in Electromagnetism*, volume 74. Springer, 2014.
- [4] P. B. Bochev and M. D. Gunzburger. *Least-Squares Finite Element Methods*, volume 166. Springer, 2009.
- [5] Ph. Bouillard. Influence of the pollution on the admissible field error estimation for FE solutions of the Helmholtz equation. *International Journal for Numerical Methods in Engineering*, 45(7):783–800, 1999.
- [6] F. Brezzi and M. Fortin. *Mixed and Hybrid Finite Element Methods*. Springer-Verlag New York, 1991.
- [7] O. Cessenat and B. Despres. Using plane waves as base functions for solving time harmonic equations with the ultra weak variational formulation. *Journal of Computational Acoustics*, 11(02):227–238, 2003.
- [8] P. G. Ciarlet. *The Finite Element Method for Elliptic Problems*, volume 40. SIAM, 2002.
- [9] Robert Davis Cook. *Concepts and applications of finite element analysis*. 1981.
- [10] M. J. Crocker. *Handbook of Acoustics*. John Wiley & Sons, 1998.
- [11] J. L. Guermond and A. Ern. *Theory and Practice of Finite Elements*. Springer, New York, 2004.
- [12] W. W. Hager. Condition estimates. *SIAM Journal on Scientific and Statistical Computing*, 5(2):311–316, 1984.
- [13] I. Harari. Dispersion, pollution, and resolution. In Steffen Marburg and Bodo Nolte, editors, *Computational acoustics of noise propagation in fluids: finite and boundary element methods*, chapter 2, pages 37–56. Springer, 2008.
- [14] A. J. Hermans. *Water Waves and Ship Hydrodynamics: An Introduction*. Springer, 2010.
- [15] M.E. Honnor, J. Trevelyan, P. Bettess, M. El-hachemi, O. Hassan, K. Morgan, and J. J. Shirron. An integration scheme for electromagnetic scattering using plane wave edge elements. *Advances in Engineering Software*, 40(1):58–65, 2009.

- [16] F. Ihlenburg. *Finite Element Analysis of Acoustic Scattering*, volume 132. Springer, 2006.
- [17] F. Ihlenburg and I. Babuska. Finite element solution of the Helmholtz equation with high wave number. Part I: The h-version of the FEM. *Computers & Mathematics with Applications*, 30(9):9–37, 1995.
- [18] F. Ihlenburg and I. Babuska. Finite element solution of the Helmholtz equation with high wave number. Part II: the hp version of the FEM. *SIAM Journal on Numerical Analysis*, 34(1):315–358, 1997.
- [19] S. G. Kelly. *Mechanical Vibrations: Theory and Applications*. Cengage Learning, 2012.
- [20] O. Laghrouche, A. El-Kacimi, and J. Trevelyan. Extension of the PUFEM to elastic wave propagation in layered media. *Journal of Computational Acoustics*, 20(02):1240006, 2012.
- [21] Z.-C. Li, T.-T. Lu, H.-Y. Hu, and A.-H.D. Cheng. *Trefftz and Collocation Methods*. WIT press, 2008.
- [22] Advanpix LLC. Multiprecision Computing Toolbox for MATLAB. Available at <http://www.advanpix.com/>, Version 3.8.1.8754.
- [23] M.S. Mahmood, O. Laghrouche, J. Trevelyan, and A. El Kacimi. Implementation and computational aspects of a 3D elastic wave modelling by PUFEM. *Applied Mathematical Modelling*, 49:568–586, 2017.
- [24] S. Marburg and B. Nolte. *Computational Acoustics of Noise Propagation in Fluids: Finite and Boundary Element Methods*, volume 578. Springer, 2008.
- [25] J. M. Melenk. *On Generalized Finite Element Methods*. PhD thesis, University of Maryland, 1995.
- [26] J. M. Melenk and I. Babuska. The partition of unity finite element method: basic theory and applications. *Computer Methods in Applied Mechanics and Engineering*, 139(1):289–314, 1996.
- [27] M.S. Mohamed, O. Laghrouche, and A. El-Kacimi. Some numerical aspects of the PUFEM for efficient solution of 2D Helmholtz problems. *Computers & Structures*, 88(23-24):1484–1491, 2010.
- [28] A. Moiola, R. Hiptmair, and I. Perugia. Plane wave approximation of homogeneous Helmholtz solutions. *Zeitschrift für angewandte Mathematik und Physik*, 62(5):809, 2011.

- [29] M. Ochmann and F. P. Mechel. Analytical and numerical methods in acoustics. In *Formulas of Acoustics*, pages 930–1023. Springer, 2004.
- [30] Karl-Gunnar Olsson and Ola Dahlblom. *Structural mechanics: modelling and analysis of frames and trusses*. John Wiley & Sons, 2016.
- [31] P. Ortiz and E. Sanchez. An improved partition of unity finite element model for diffraction problems. *International Journal for Numerical Methods in Engineering*, 50(12):2727–2740, 2001.
- [32] A. A. Samarskii. *The Theory of Difference Schemes*, volume 240. CRC Press, 2001.
- [33] J. Shen, T. Tang, and L.-L. Wang. *Spectral Methods: Algorithms, Analysis and Applications*, volume 41. Springer, 2011.
- [34] I. Singer and E. Turkel. High-order finite difference methods for the Helmholtz equation. *Computer Methods in Applied Mechanics and Engineering*, 163(1-4):343–358, 1998.
- [35] Pavel Solín, Tomáš Vejchodský, and Martin Žitka. Orthogonal hp-fem for elliptic problems based on a non-affine concept. In *Numerical Mathematics and Advanced Applications*, pages 683–690. Springer, 2006.
- [36] T. Strouboulis, I. Babuska, and R. Hidajat. The generalized finite element method for Helmholtz equation: theory, computation, and open problems. *Computer Methods in Applied Mechanics and Engineering*, 195(37-40):4711–4731, 2006.
- [37] L. L. Thompson. A review of finite-element methods for time-harmonic acoustics. *The Journal of the Acoustical Society of America*, 119(3):1315–1330, 2006.
- [38] C. Wenterodt and O. Von Estorff. Optimized meshfree methods for acoustics. *Computer Methods in Applied Mechanics and Engineering*, 200(25-28):2223–2236, 2011.